Delft University of Technology

Control Engineering
SC42095

Assignment: Bi-wing aircraft

Authors:
David Chen (5705762)

March 4, 2024

Contents

1 Continuous-time Control

In this chapter, controllers are designed in continuous time to achieve reference tracking and disturbance rejection. To do so, the dynamic of the original system is analyzed in section 1.1. In Section 1.2, a PD controller is designed to achieve reference tracking. A PID controller for disturbance rejection is designed in Section 1.3.

1.1 Analysis of original system

The transfer function of the system is given as

$$G(s) = \frac{4000}{s(s+10)(s+20)} \tag{1}$$

it can be drawn from equation 1 that the original system has poles of $0, -10, -20$ and without zeros. visualization of the system depicted by equation 1 is shown below.

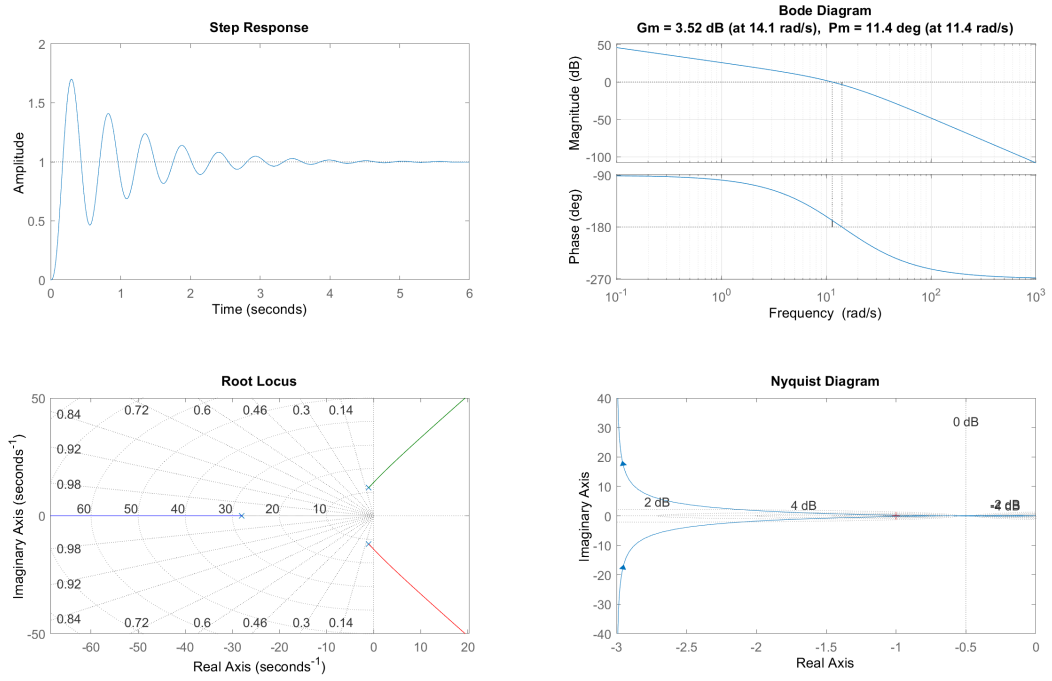

Figure 1: The step response, bode diagram, root locus, and Nyquist plot of the system

Define the open-loop transfer function as $L(s)$, the corresponding closed-loop transfer function with a feedback gain of 1 can be acquired as

$$G_{cl}(s) = \frac{Y(s)}{U(s)} = \frac{L(s)}{1+L(s)} = \frac{4000}{s^3 + 30s^2 + 200s + 4000} \tag{2}$$

From equation 2, the transfer function of error can be acquired as

$$G_{error}(s) = \frac{E(s)}{U(s)} = \frac{1}{1+L(s)} = \frac{s(s+10)(s+20)}{s(s+10)(s+20) + 4000} \tag{3}$$

The step response of the closed-loop system indicates that it is stable without any controller involved. Moreover, based on equation 3, and the final value theorem $\lim_{t\to\infty} e(t) = \lim_{s\to 0} se(s)$, it can be concluded that there is no steady-state error in terms of the step response. Hence, an integrator won't be necessary in the design. Additionally, more insights can be acquired from the bode diagram and the root locus: the positive value (11.4^o) of Phase Margin (PM) indicates stability. However, the Gain Margin (GM), which measures the amount of gain that can be added to the system before it becomes unstable, with a value of 3.52 dB indicates that a large gain cannot be added. This can also be seen from the root locus that a large gain will result in the poles moving to the right-hand side, leading to instability.

1.2 Question 1: Reference Tracking

The goal of this chapter is to design a controller such that a reference set-point step has a fast response. Three requirements are given for the set-point step reference tracking.

- Minimal settling-time
- Overshoot $< 5\%$
- Zero steady-state error

From the analysis in the previous chapter, the 3^{rd} requirement is already achieved. To design the controller, the original system is simplified by neglecting the non-dominate pole of -30 since the effect of transients of the pole that is far away from the dominant poles decayed over time [3]. Subsequently, the simplified closed-loop system becomes.

$$G(s) = \frac{4000}{s^2 + 10s + 4000} \tag{4}$$

which is the same form as the standard second-ordered system

$$G(s) = \frac{\omega_n^2}{s^2 + 2\xi\omega_n + \omega_n^2} \tag{5}$$

The system described by 5 has two poles, $P_{1,2} = \sigma \pm j\omega_d = -\xi\omega_n \pm j\omega_n\sqrt{1-\xi^2}$. Defining the imaginary part $\omega_d = \omega_n\sqrt{1-\xi^2}$, the rise time T_r, settling time T_s, and overshoot M_p can be represented by the variables in terms of ω_n, ξ, and ω_d.

1. Rise-time $T_r = \frac{\pi - arccos(\xi)}{\omega_d}$
2. Settling time $T_s = \frac{4}{\xi\omega_n}$
3. Maximum overshoot $M_p = e^{\frac{-\pi\xi}{\sqrt{1-\xi^2}}} \times 100\%$

Combined with the representation of poles, to achieve a short settling time, the real part of the controlled system's poles should be made large while the damping ratio ξ should not be larger than 0.69 to guarantee that the overshoot is less than 5%.

The above analysis offers great insights into tuning the PID controller, one of the most commonly used controllers in the industry for its robustness and low implementation cost. The general mathematical expression of the PID controller is defined as

$$PID = K_p + \frac{K_i}{s} + K_d\frac{s}{T_f s + 1} \tag{6}$$

By elevating the proportional term K_p, the rise time T_r of the system diminishes. However, an excessively high value of K_p can jeopardize stability. Term K_i can eliminate the steady-state error, increasing too much results in introducing overshoots and oscillations that could break the stability. The derivative term K_d plays a role in mitigating oscillations and curtailing overshoots by instilling damping characteristics.

Previous analysis indicates that an K_i term won't be necessary. Hence, P and PD controllers are designed to reach the performance goals at a minimal cost. Based on equation 6, PD controller is defined as

$$PD = k_p + K_d\frac{s}{T_f s + 1} = \frac{(K_d + K_p T_f)s + K_p}{T_f s + 1} \tag{7}$$

Equation 7 can be rewritten into the form of a lead-lag compensator, which yields the following equation

$$C(s) = K_c\frac{s + z_0}{s + p_0} = \frac{K_d + K_p T_f}{T_f}\frac{s + \frac{K_p}{K_d + K_p T_f}}{s + \frac{1}{T_f}} \tag{8}$$

When $z_0 > p_0$, the compensator introduces lead compensation, acting as a high-pass filter that imparts a higher crossover frequency to the system $C(s)G(s)$. This leads to an expanded bandwidth, culminating in a swifter response. In the time domain, the introduction of a lead compensator shifts the root locus further to

the left, signifying increased stability. This conclusion is drawn from the definition of the asymptotes and the intersection points of the root locus.

$$a = \frac{\sum p - \sum z}{num(p) - num(z)} \tag{9}$$

by adding a larger z, the numerator of equation 9 becomes smaller, or more negative, while the denominator remains the same.

To design the optimal controller, a decent K_p is first tuned, and then followed by K_d.

1.2.1 P controller

When $P = 1$, indicating no control action is applied to the system, the gain margin (GM), phase margin (PM), and settling time T_s of the system are $3.52dB$, 11.4^o, and $3.756s$ individually. When increasing the K_p value to 1.5, the system starts to oscillate. And it is found that if $K_p > 1.5$, the stability of the system will break. When decreasing the K_p value to 0.8, the gain margin (GM), phase margin (PM), and settling time T_s of the system are $5.46dB$, 18.1^o, and $2.4393s$ respectively, representing more robust stability and smaller settling time T_s but larger rising time T_r. The above observation agrees with the theoretical analysis.

After a few tuning, the optimal K_p is found at the value of 1.5. Visualization of the closed-loop system is shown in figure 2.

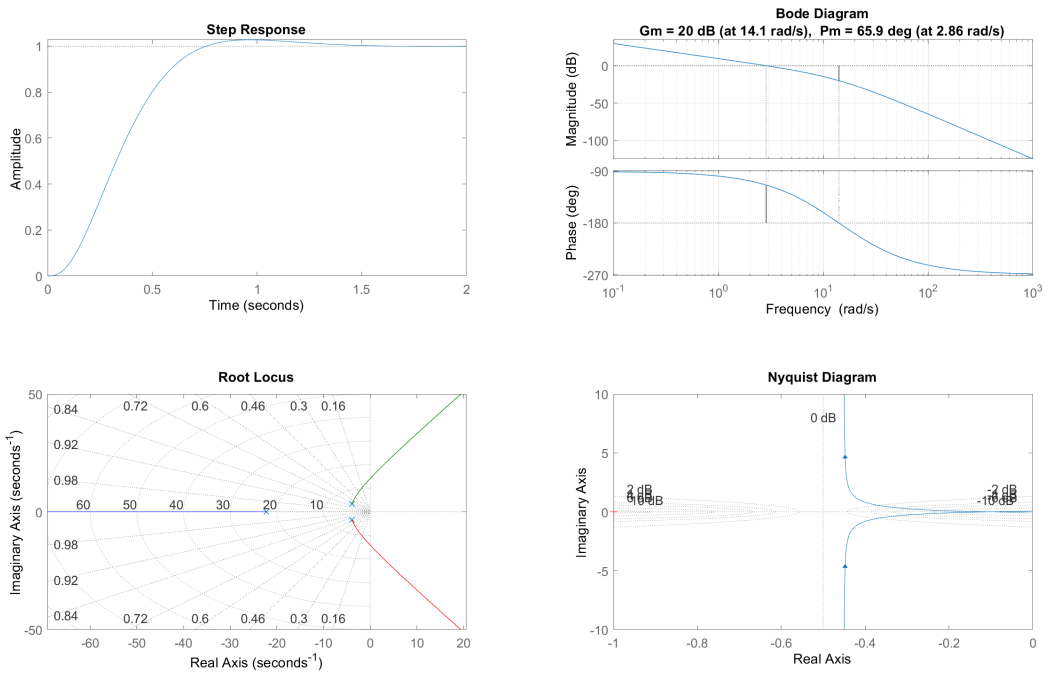

Figure 2: The step response, bode diagram, root locus, and Nyquist plot of the P-controlled system

After applying the designed P controller, the closed-loop poles of the system are $-22.2120, -3.894 \pm 3.4423j$, indicating stability. Settling time T_s and maximum overshoot M_p is $1.1493s$ and 2.7633% respectively.

1.2.2 PD controller

Based on the control effect of a P controller, it can be observed that the overshoot of the system can be eliminated while the settling time could be decreased. To do so, a D controller is added. The PD controller, or the lead-lag compensator added has a mathematical definition as equation 8, whereas T_f is the first-order derivative filter time constant. A lead-lag compensator has a bode diagram as figure 3 shows, this resembles the bode diagram of a high-pass filter.

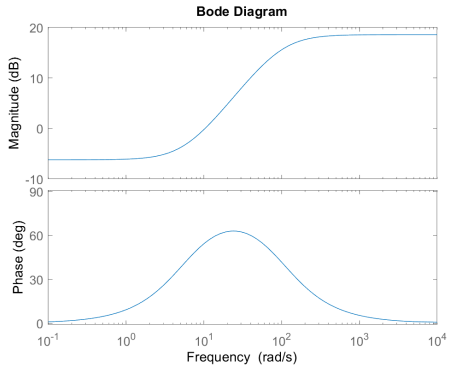

Figure 3: Bode diagram of a lead-lag compensator

If rewrite the lead-lag compensator again as

$$C(s) = K_c\alpha\frac{Ts+1}{\alpha Ts+1} \tag{10}$$

with $\alpha = \frac{T_f K_p + K_d}{T_f K_p}$. The frequency where the phase reaches its peak equals $\omega_{max} = \frac{1}{\sqrt{\alpha}T}$ with the largest phase $\phi = arcsin(\frac{\alpha-1}{\alpha+1})$. In order to make the PD controller closer to ideal while feasible, T is set as 100, and $\alpha = 9$ to satisfy the phase margin. After several tuning based on the K_p acquired by the P controller, the controller effect of the tuned PD controller is shown below.

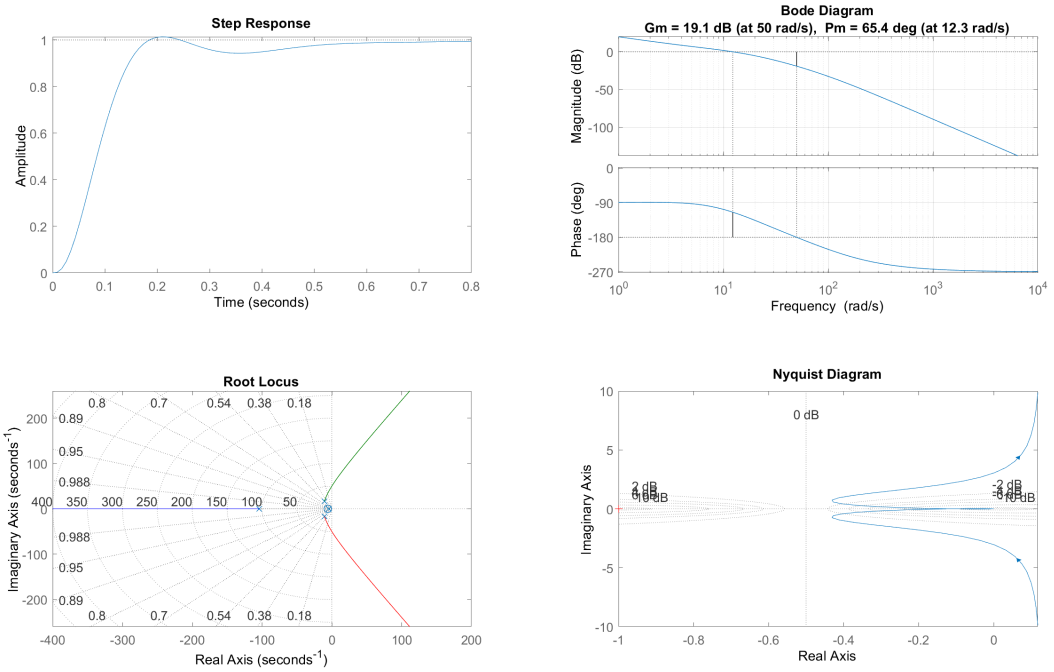

Figure 4: Visualization of the PD-controlled with $K_p = 0.49$, $K_d = 0.08$, and $T_f = 0.01$

Therefore, the lead-lag compensator is defined as

$$C(s) = \frac{8.49s + 49}{s + 100} \tag{11}$$

with the controller system having an overshoot of 1.3648%, settling time of $0.5212s$, and zero-steady-state error.

1.3 Question 2: Disturbance Rejection

In this question, a disturbance q is added to the system while reference $r = 0$. The goal of the controller is to achieve

- Zero offset caused by the disturbance
- Minimal amplitude of output y caused by disturbance q
- Minimal duration of the disturbance

The first requirement is analyzed. Based on the block diagram given in the question, the transfer function from disturbance q to output y can be acquired as

$$G_d(s) = \frac{Y(s)}{Q(s)} = \frac{G(s)}{1 + C(s)G(s)} \tag{12}$$

based on the finite value theorem, for a given disturbance q, the output from the system is

$$\lim_{t\to\infty} y(t) = \lim_{s\to 0} sY(s) = \lim_{s\to 0} sQ(s)\frac{G(s)}{1 + G(s)C(s)} = \lim_{s\to 0} sQ(s)\frac{1}{\frac{1}{G(s)} + C(s)} \tag{13}$$

Given open loop transfer function $G(s)$ defined in equation 1, the term $\frac{1}{G} = 0$ when $s = 0$. Thus, for $y(t)$ to equal 0 for any disturbance $q(t)$, controller $C(s)$ needs to contain an integrator to provide a $\frac{1}{s}$ term. Otherwise, a step disturbance would result in an offset. Hence, a PID controller needs to be used to achieve the requirements for disturbance rejection. Since a physically realizable controller needs to be designed, the form of PID is the same as equation 6.

To achieve a fast settling time, a high bandwidth is expected. However, unlike reference tracking, a faster disturbance rejection requires more gain inside the bandwidth assuming the control bandwidth is fixed [3]. Therefore, this can only be achieved by increasing the slope near the crossover frequency in the bode diagram. Subsequently, it requires a smaller phase margin for a larger slope even though it comes at the expense of more overshoot in the response to setpoint changes when it comes to reference tracking. Hence, when tuning the PID controller using loop shaping, we expected to have a positive gain margin, a small and positive phase margin, and a high bandwidth for open loop system $G(s)C(s)$.

To make the PID controller realizable, sampling time T_f is kept as 0.01 like the previous design. A $k_i = 1$ is added to the previous controller, and the effect of disturbance rejection is shown in figure 5.

In figure 5, the bode diagram of $G(s)C(s)$, $G(s)$, and $C(s)$ are all plotted in the same figure, providing insights into the influence of a PID controller on the frequency response. Moreover, the turning point in the bode diagram of a PID controller is determined by the position of the zeros of equation 36. To attain a favorable outcome in loop shaping, the position of the zeros should be placed so that the turning point is a bit left to the current one to achieve a small phase margin. To reduce the phase margin, k_p, k_i, and k_d can all be increased. However, increasing one parameter too much will lead to unfavorable system behaviors. For example, increasing k_p will give the system a higher bandwidth but also a high amplitude of output.

After several tuning attempts, a satisfactory outcome has been achieved, as evidenced by the observed control effect presented in figure 6.

To achieve a lower output amplitude and smaller settling time, k_p, k_i, and k_d are increased for a few attempts for tuning while ensuring a positive gain margin and phase margin. The final controller has a disturbance rejection effect in the figure 7.

To sum up, the final designed controller has the parameters of $k_p = 2.9, k_i = 15, k_d = 0.3$, and $T_f = 0.01$. The transfer function of the corresponding PID controller can be obtained by substituting the determined values into 6.

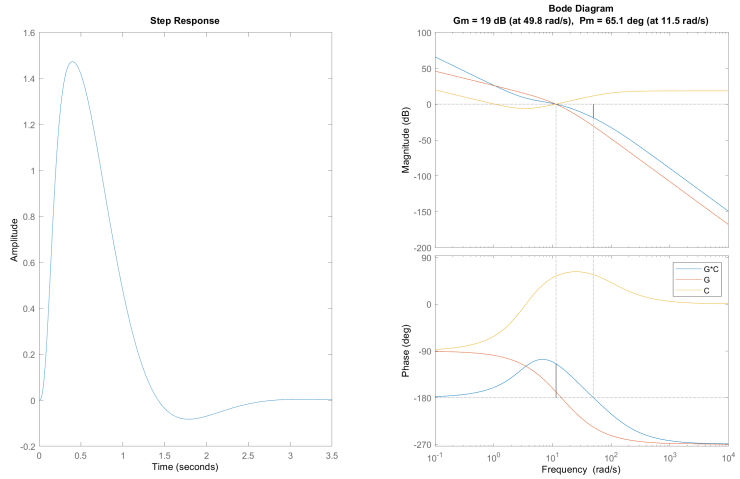

Figure 5: Previous controller with $k_i = 1$

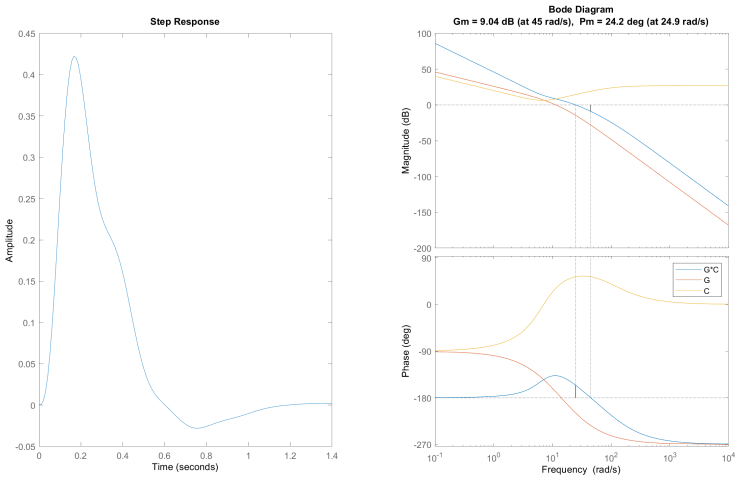

Figure 6: Disturbance rejection effect of $k_p = 2, k_i = 10, k_d = 0.2$

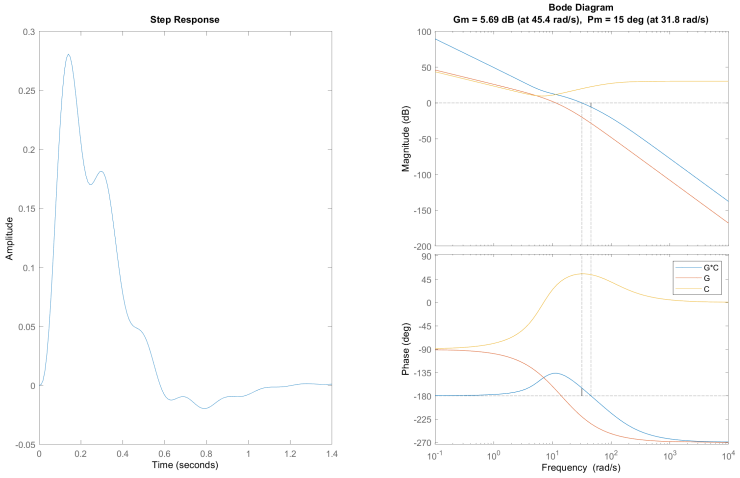

Figure 7: Disturbance rejection effect of $k_p = 2.9, k_i = 15, k_d = 0.3$

2 Discrete-time Control

In this chapter, the continuous system is discretized, and the resulting discretized system is analyzed. Furthermore, a discrete closed-loop feedback controller (PID) and a state feedback controller are designed.

2.1 Question 3: Discrete State Space Model

The state-space representation of equation 1 can be acquired by using the built-in function $tf2ss$ in Matlab, which yields

$$\begin{bmatrix} \dot{x_1} \\ \dot{x_2} \\ \dot{x_3} \end{bmatrix} = \begin{bmatrix} -30 & -200 & 0 \\ 1 & 0 & 0 \\ 0 & 1 & 0 \end{bmatrix} \begin{bmatrix} x_1 \\ x_2 \\ x_3 \end{bmatrix} + \begin{bmatrix} 1 \\ 0 \\ 0 \end{bmatrix} u \tag{14}$$

$$y = \begin{bmatrix} 0 & 0 & 4000 \end{bmatrix} \begin{bmatrix} x_1 \\ x_2 \\ x_3 \end{bmatrix} + \begin{bmatrix} 0 \end{bmatrix} u \tag{15}$$

The next step will be to choose the appropriate sampling frequency ω_s. A too-low ω_s leads to losing important information, while a too-high ω_s increases the computational burden on the processor. The discretization method used in this section is ZOH, standing for zero-order hold, which assumes that the system holds the value until receiving the next sample.

The first attempt to choose ω_s is based on the open-loop rise time T_r, in which the sampling time T_s can be determined by $\frac{T_r}{N}$ with N being an integer between 4 to 10. However, the unstable behavior of the open-loop system made this method impossible to use. Hence, ω_s is chosen based on the bandwidth ω_b with the relation that

$$\omega_s \approx 20\omega_b \tag{16}$$

so that ω_s is fast enough to capture the dynamic of the system.

A second-order system approximation is often used and says that the bandwidth frequency ω_b equals the frequency at which the open-loop magnitude response is between -6 and -7.5 dB in a real engineering scenario [2]. From figure 1, it can be acquired that $\omega = 16.4(rad/s)$ when magnitude equals $-6dB$. Hence, based on

$$\omega_s \approx 20\frac{(\omega|_{-6dB})}{2\pi} \tag{17}$$

the sampling frequency is chosen as $\omega_s = 50Hz$.

Finally, the discretized matrices can be acquired by

$$\Phi = e^{Ah} \text{ and } \Gamma = \int_0^h d^{As} ds B \tag{18}$$

resulting in the discrete state space representation:

$$\begin{bmatrix} x_1(k+1) \\ x_2(k+1) \\ x_3(k+1) \end{bmatrix} = \begin{bmatrix} 0.5219 & -2.968 & 0 \\ 0.01484 & 0.9671 & 0 \\ 0.0001643 & 0.01977 & 1 \end{bmatrix} \begin{bmatrix} x_1(k) \\ x_2(k) \\ x_3(k) \end{bmatrix} + \begin{bmatrix} 0.01484 \\ 0.0001643 \\ 1.151e-06 \end{bmatrix} u(k) \tag{19}$$

$$y(k) = \begin{bmatrix} 0 & 0 & 4000 \end{bmatrix} \begin{bmatrix} x_1(k) \\ x_2(k) \\ x_3(k) \end{bmatrix} + \begin{bmatrix} 0 \end{bmatrix} u(k) \tag{20}$$

with the definition of state

$$\begin{bmatrix} x_1 \\ x_2 \\ x_3 \end{bmatrix} = \begin{bmatrix} \text{heading angular acceleration} \\ \text{heading angular speed} \\ \text{heading angular position} \end{bmatrix}$$

2.2 Question 4: Discretize Controllers

In the previous section, the system was subjected to discretization. In the present section, I applied suitable discretization methods to discretize the controllers previously formulated for reference tracking and disturbance rejection.

2.2.1 Reference tracking

Matlab offers 6 different ways of discretization: 'zoh', 'foh', 'impulse', 'tustin', 'matched', and 'least-squares' in function **c2d**. For this assignment, three methods, namely 'zoh', 'tustin', and 'matched', are selected for comparison. This selection is grounded in the popularity of the first two methods and the effectiveness of the third method, which offers a notable alignment between poles and zeros of $H(s)$ in s-domain with the corresponding poles and zeros of $H(z)$ in z-domain. Note that in real engineering scenarios, when designing a controller, it is common practice for the sampling frequency of the controller to be higher than that of the system. This is often implemented to attain a finer resolution for control actions. Nevertheless, for this assignment, the sampling frequency ω_s is upheld at $50Hz$ to economize on the expense associated with developing an additional sampling circuit.

The reference tracking performances of discretized controllers using different discretization methods are depicted in figure 8

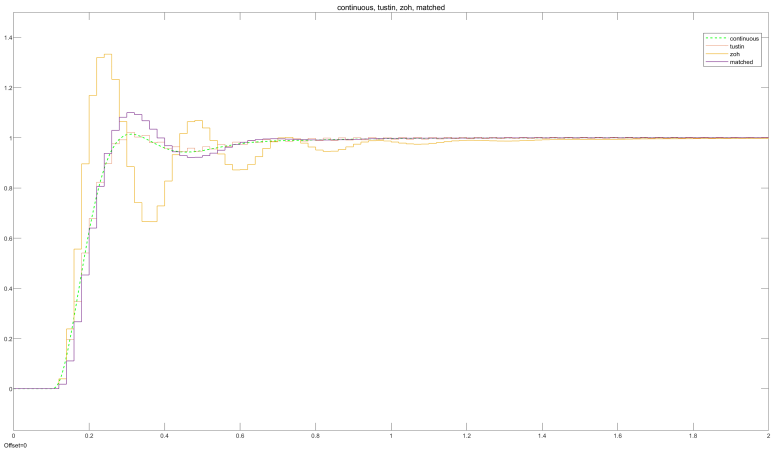

Figure 8: Control effect of the discrete controller using 'zoh', 'tustin', and 'matched'

From the figure, it can be observed that 'tustin' has the best behavior followed by 'matched' and 'zoh'. **Hence, 'tustin' is chosen as the discretization method.** To explain the difference, the bode diagram of the 3 discrete controllers is plotted in figure 9.

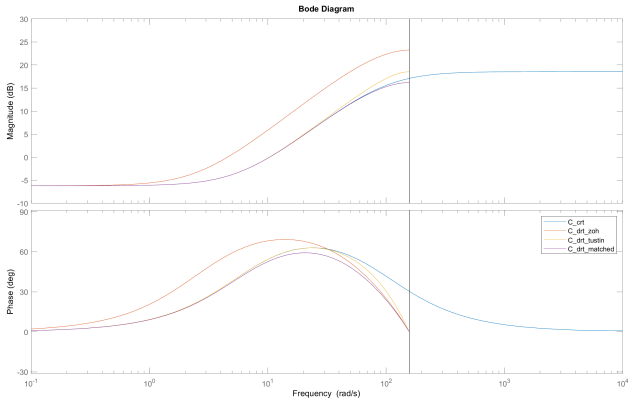

Figure 9: The bode diagram of the discrete controller using 'zoh', 'tustin', and 'matched'

The mismatched behavior of the controller discretized by the 'zoh' method can be attributed to the discrepancies in the bode diagram in terms of magnitude and phase. Furthermore, compared to the 'matched' method, the phase diagram of the 'tustin' method resembles the continuous system the most before the crossover frequency of $C(s)G(s)$. $C(s)$ represents the designed continuous PD controller.

To sum up, the discretized controller for reference tracking is

$$C(z) = k_p + k_d \frac{1}{T_f + \frac{T_s}{2}\frac{z+1}{z-1}} \tag{21}$$

with $k_p = 0.49$, $k_d = 0.08$, $T_f = 0.01$, and $T_s = 0.02$ using the 'tustin' method.

2.2.2 Disturbance rejection

The same operation is performed for disturbance rejection, resulting in the performance shown in figure 10 with the discrete controller defined as

$$C(z) = k_p + k_i \frac{T_s(z+1)}{2(z-1)} + k_d \frac{1}{T_f + \frac{T_s}{2}\frac{z+1}{z-1}} \tag{22}$$

with $k_p = 2.9$, $k_d = 15$, $k_d = 0.3$, $T_f = 0.01$, and $T_s = 0.02$.

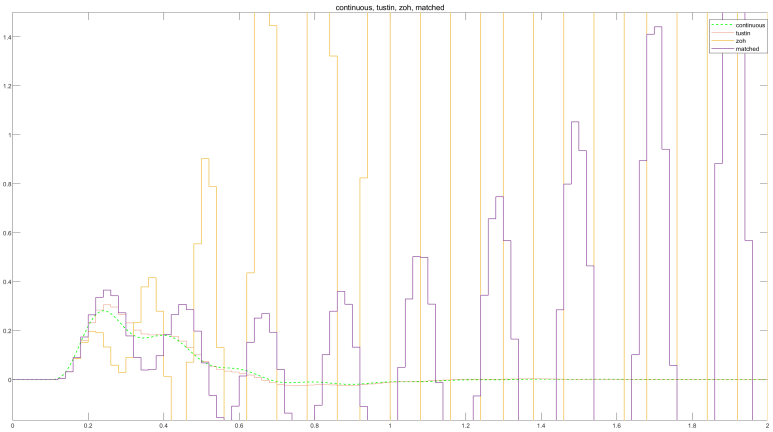

Figure 10: Disturbance rejection performance of controller using 'zoh', 'tustin', and 'matched' method

Lastly, it is discovered that by choosing a higher sampling frequency, say, $\omega_s = 100Hz$, a better performance for controllers discretized by 'zoh' and 'matched' methods could be observed. The performance of disturbance rejection by controllers discretized using 'zoh', and 'matched' methods with sampling frequency $\omega_s = 100Hz$ is shown in figure 11.

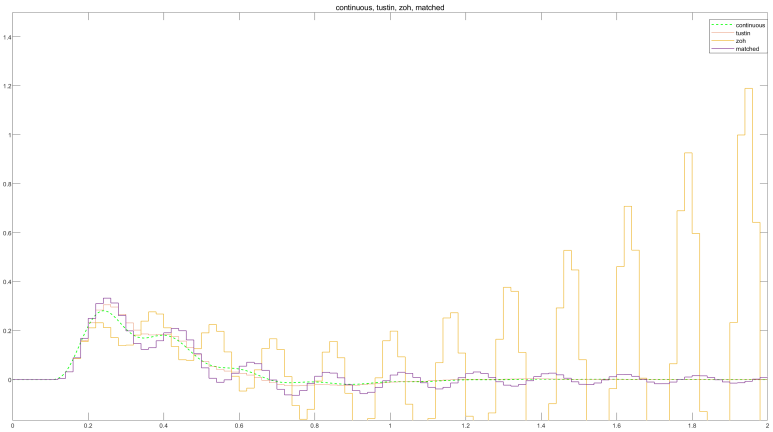

Figure 11: Disturbance rejection performance of controller discretized using 'zoh', 'tustin', and 'matched' methods

From the visualization, it can be observed that, by increasing ω_s, the performance of controllers adopted either 'matched' or 'tustin' improved. However, the 'zoh' discretized controller exhibits persistent oscillations for disturbance rejection across varying sampling frequencies.

2.3 Question 5: Discrete Pole Placement

In this question, a servo controller is built to track reference signals based on the discrete pole placement. The goal is to make the states and the outputs of the system respond to command signals in a specified way [1].

2.3.1 General Design

The first thing on the checklist for the pole placement is to check the controllability of the system. Subsequently, the controllability matrix of the discrete system is constructed as equation 23,

$$\begin{bmatrix}\Gamma & \Phi\Gamma & \Phi^2\Gamma\end{bmatrix} \tag{23}$$

which has the rank of 3. Thus, the system is controllable, meaning that the desired closed-loop system behavior can be achieved through the application of control inputs, offering a crucial requirement for pole placement.

An approach to achieve reference tracking for the discrete system is to design input u as

$$u(k) = -Kx(k) + K_r r(k) \tag{24}$$

where $u(k)$, $r(k)$, and K denote the controlled input, reference input, and feedback gain separately [1]. Subsequently, since $D = 0$, the state space representation of the discrete system becomes

$$\begin{aligned} x(k+1) &= \Phi x(k) + \Gamma u(k) \\ y(k) &= Cx(k) \\ u(k) &= -Kx(k) + K_r r(k) \end{aligned}$$

When selecting the position of poles, an indirect method is adopted, involving the initial choice of poles in the continuous-time domain, followed by discretizing them to the discrete-time domain. This method operates under the assumption that the system's behavior undergoes minimal alteration during the discretization process. Furthermore, sampling time T_s is set as 0.02, the same for discretizing the system and controllers. The overarching design procedure can be succinctly summarized as follows

1. Select poles in the s-domain
2. Find the corresponding poles in the z-domain by $z = e^{sT_s}$
3. Find the feedback gain K by using the *place* command, and obtain the feedforward gain by *dcgain* command
4. Construct Simulink models for simulations
   - K in figure 12 stands for feedback gain obtained from pole placement
   - $kDiscF$ in figure 12 denotes the feedforward gain, which is defined as the inverse of the DC gain of the closed-loop system

The general form of the block diagram used for simulating the state space system is illustrated in figure 12

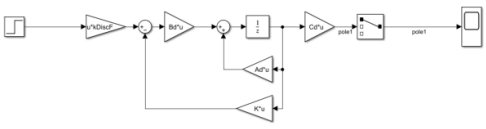

Figure 12: Block diagram of the discrete system integrated a servo controller

2.3.2 Selection of Poles

During the analysis, the 3 poles of the system can be categorized into two groups: a negative real pole, and a pair of conjugated poles. The idea is similar to the lower-order estimation, involving first settling the conjugated poles, which are also the dominant poles, to determine the system's primary behavior. Lastly, the negative real pole is utilized to accelerate the response.

In chapter 1.2, given the requirement of the overshoot, the maximum value of the damping ratio ζ is calculated as 0.69. This influences the choosing of poles in terms of their angle with the real axis θ based on $\zeta = cos(\pi - \theta)$.

Lastly, when selecting the modulus of the conjugated pole pair, it is crucial to ensure that the real part of these poles does not exceed the negativity of the single real negative pole. This precaution is taken to guarantee that the latter pole represents the speed of the system response.

2.3.3 Result

Based on the previous analysis, 4 pairs of poles are selected for testing. Step responses are illustrated in the figure 13.

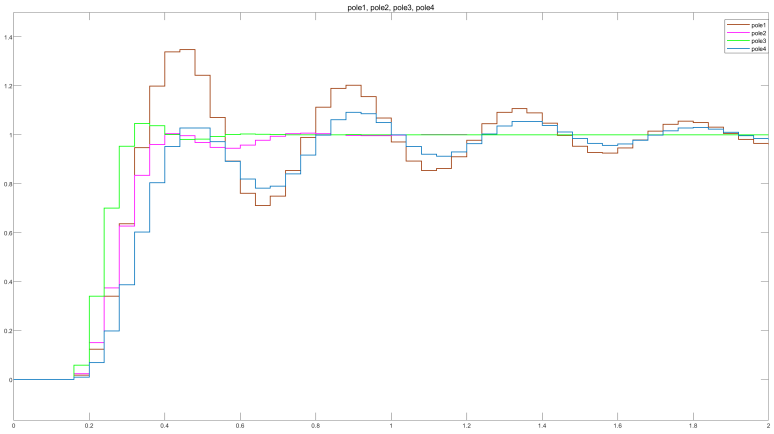

Figure 13: Step response of systems controlled by four state feedback servo controllers

The corresponding locations of poles, closed-loop system performances, and feedback gain K are also listed in the table 1.

	Continuous Pole	Discrete Pole	ζ	T_r(s)	Overshoot(%)	K(discrete)
Pole4	-10, -3±27.94i	0.8187, 0.8±0.5i	0.1068	0.06	35.91	[0.2190 0.0010 3.9996]
Pole1	-20, -3±27.94i	0.6703, 0.8±0.5i	0.1068	0.0863	9.309	[0.2071 -0.0013 2.1991]
Pole2	-17, -12.3574±34.7369i	0.7, 0.6±0.5i	0.3352	0.0748	0.67	[0.3858 0.0053 5.1455]
Pole3	-35, -22.29±44.8028i	0.5, 0.4±0.5i	0.4454	0.0506	5.00	[0.6961 0.0114 12.8463]

Table 1: Different choices of poles

From the figure, pole4 and pole1 have serious underdamped behavior given the damping ratio ζ. By increasing the damping ratio of the conjugated pole more towards the critically damped situation, the system has better behavior with fewer oscillations. Moreover, by placing the poles further negatively in the s-domain, correspondingly to placing the pole closer to the origin in the z-domain, the system has a faster response. However, note that the best pole pair has the biggest feedback gain K. Therefore, a trade-off must be sought in terms of implementation. Given the absence of physical constraints, the final pole is positioned close to the origin.

Continuous Pole	Discrete Pole	ζ	T_r(s)	Overshoot(%)	K(discrete)
-35, -22.29±44.8028i	0.5, 0.4±0.5i	0.4454	0.0506	5.00	[0.6961 0.0114 12.8463]

2.4 Question 6: Observer Design

In the real engineering scenario, it is not always a situation that all states can be observed. Thus, an observer is designed to solve this problem.

2.4.1 Reference tracking

Before designing the observer, the observability of the system is first examined. The observable matrix 25 is constructed as equation 25. For the given system, the observable matrix has a rank of 3, indicating the observability. Thus, in theory, there is no need to build an observer. However, an observer is still built for comparison.

$$W_o = \begin{bmatrix} C_d \\ C_d\Phi \\ C_d\Phi^2 \end{bmatrix} \tag{25}$$

The observer gain is denoted by L, and the estimated state and output are denoted by $\hat{x}$ and $\hat{y}$. Consequently, the system with an observer and a servo controller can be described as:

$$\begin{aligned} x(k+1) &= \Phi x(k) + \Gamma u(k) \\ \hat{x}(k+1) &= \Phi\hat{x}(k) + \Gamma u(k) + L(y(k) - \hat{y}(k)) \\ y(k) &= Cx(k) \\ u(k) &= -Kx(k) + Kr(k) \end{aligned}$$

Based on the state space representation, the error e_x between the real state and estimated state is expressed by equation 26

$$e(k+1) = x(k+1) - \hat{x}(k+1) = (\Phi - LC)e(k) \tag{26}$$

Wrap up all the above representations, the augmented state space representation of the system can be expressed as:

$$\begin{aligned} \begin{bmatrix} x(k+1) \\ \hat{x}(k+1) \end{bmatrix} &= \begin{bmatrix} \Phi - \Gamma K & \Gamma K \\ 0 & \Phi - LC \end{bmatrix} \begin{bmatrix} x(k) \\ \hat{x}(k) \end{bmatrix} + \begin{bmatrix} K_r\Gamma \\ 0 \end{bmatrix} r \\ y(k) &= \begin{bmatrix} C - DK \\ DK \end{bmatrix} \begin{bmatrix} x(k) \\ \hat{x}(k) \end{bmatrix} \end{aligned}$$

After constructing the augmented system, the next step is to determine the observer gain L. Pole placement is utilized for designing the observer based on the *acker* function. There are two requirements for the design of the observer:

1. Matrix $\Phi - LC$ should be Hurwitz to guarantee zero convergence of the error e.
2. Observer poles should be placed in a position that guarantees a faster response than the system response to capture its dynamics.

Based on the above requirements, the observer poles are chosen by subtracting 0.1 and 0.2 from both real and imaginary parts of the closed-loop poles based on the relationship between the position of the poles and the system's response speed. Note that the sampling time Ts is set as 0.02 the same as previous designs.

System Continuous Pole	System Discrete Pole	Observer Continuous Pole	Observer Discrete Pole
-35, -22.29±44.8028i	0.5, 0.4±0.5i	-45.8145, -51.0055±29.4001i	0.4, 0.3±0.2i

Figure 14 shows x and $\hat{x}$, from which one can notice that the observer succeeds in capturing the dynamic of the system.

Finally, an initial value of 0.5 is added to the reference of the heading of the bi-wing aircraft. The error between the estimated state $\hat{x}$ and real state x is visualized in figure 15a. Moreover, the reference tracking performance is shown in figure 15b.

From the visualization, the system with an observer succeeds in following the given reference with a non-zero initial value. However, it can be noticed that there is a bigger drop on x_3, denoting the heading of the aircraft, at the start of the simulation for the system with an observer compared to the system without. The explanation for this drop could be that the observer fails to capture the dynamic of x_3 before 0.2s. The plot of error, as well as the visualization of x and $\hat{x}$ validate this argumentation. In reality, this effect could be catastrophic. Thus, improvements can be made by

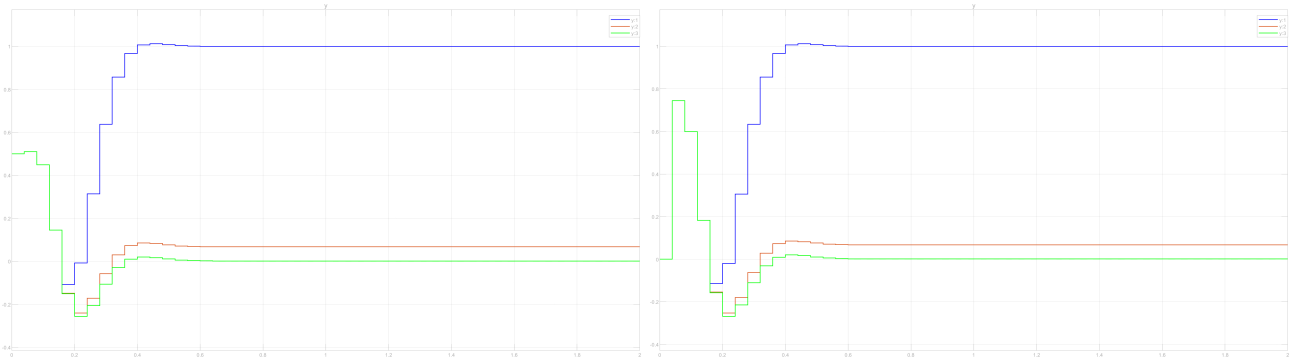

(a) x (b) $\hat{x}$

Figure 14: Real state and estimated state from the observer

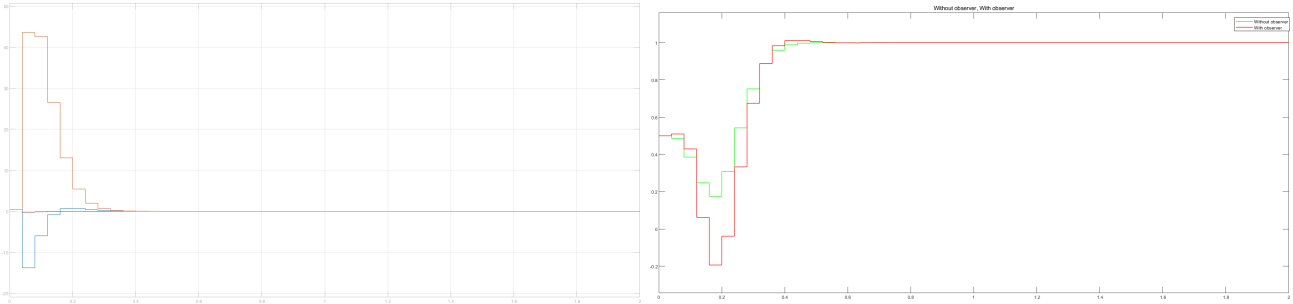

(a) State Error (b) Reference tracking based on the designed observer

Figure 15: State Errors and Reference Tracking

- Fine-tuning the observer for a faster response.
- Add a yaw damper to the aircraft to circumvent this effect.
- Eliminate the use of observers by upgrading the flight control system.

2.4.2 Disturbance rejection

In this section, a step disturbance $d(k)$ is added to the system, as figure 16 illustrates

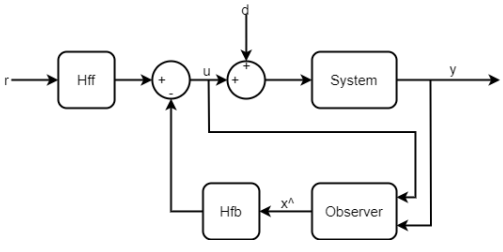

Figure 16: Block diagram of the system for disturbance rejection with an observer

To assess the necessity for adding an integrator, a disturbance $d(k)$ with the magnitude of 1 and activation time at $5s$ is added. This addition results in the system failure in tracking the reference r. Thus, the system needs to be augmented with integral action. The definition of the augmented state is derived from the input of the system, which has changed from $u(k)$ to $u^{'}(k) = u(k) + \omega(k)$. Subsequently, the state space of the system

becomes

$$\begin{bmatrix} x(k+1) \\ \omega(k+1) \end{bmatrix} = \begin{bmatrix} \Phi & \Gamma \\ 0 & 1 \end{bmatrix} \begin{bmatrix} x(k) \\ \omega(k) \end{bmatrix} + \begin{bmatrix} \Gamma \\ 0 \end{bmatrix} u(k)$$
$$y(k) = \begin{bmatrix} C & 0 \end{bmatrix} \begin{bmatrix} x(k) \\ \omega(k) \end{bmatrix}$$
$$u(k) = \begin{bmatrix} -k & -k_\omega \end{bmatrix} \begin{bmatrix} x(k) \\ \omega(k) \end{bmatrix} + K_r r(k)$$

in which $[-k, -k_\omega]$ is defined as the feedback gain matrix K. To reject the disturbance, k_ω is chosen as 1. Apart from the feedback gain, the observer gains matrix L is augmented as $[L, L_\omega]$ to estimate both x and ω. The state space representation of the augmented system is finally obtained as

$$\begin{bmatrix} x(k+1) \\ \omega(k+1) \\ \hat{x}(k+1) \\ \hat{\omega}(k+1) \end{bmatrix} = \begin{bmatrix} \Phi & \Gamma & 0 & 0 \\ 0 & 1 & 0 & 0 \\ LC & 0 & \Phi - LC & \Gamma \\ L_\omega C & 0 & -L_\omega C & 1 \end{bmatrix} \begin{bmatrix} x(k) \\ \omega(k) \\ \hat{x}(k) \\ \hat{\omega}(k) \end{bmatrix} + \begin{bmatrix} \Gamma \\ 0 \\ \Gamma \\ 0 \end{bmatrix} u(k)$$
$$y(k) = \begin{bmatrix} C & 0 & 0 & 0 \end{bmatrix} \begin{bmatrix} x(k) \\ \omega(k) \\ \hat{x}(k) \\ \hat{\omega}(k) \end{bmatrix}$$
$$u(k) = \begin{bmatrix} -k & -k_\omega \end{bmatrix} \begin{bmatrix} \hat{x}(k) \\ \hat{\omega}(k) \end{bmatrix} + K_r r(k)$$

The discrete pole of the observer is placed at $[0.1, 0.15 \pm 0.2i, 0.6]$ so that the augmented term has a slower response compared to other terms in the observer. The disturbance rejection performance of systems with and without the augmented state is shown in figure 17, from which it can be noticed that the augmented system succeeds in tracking the reference $r(k)$ under the influence of the input disturbance $d(k)$. On the contrary, the system without augmentation integrator action has a large stable state error after the input disturbance involved.

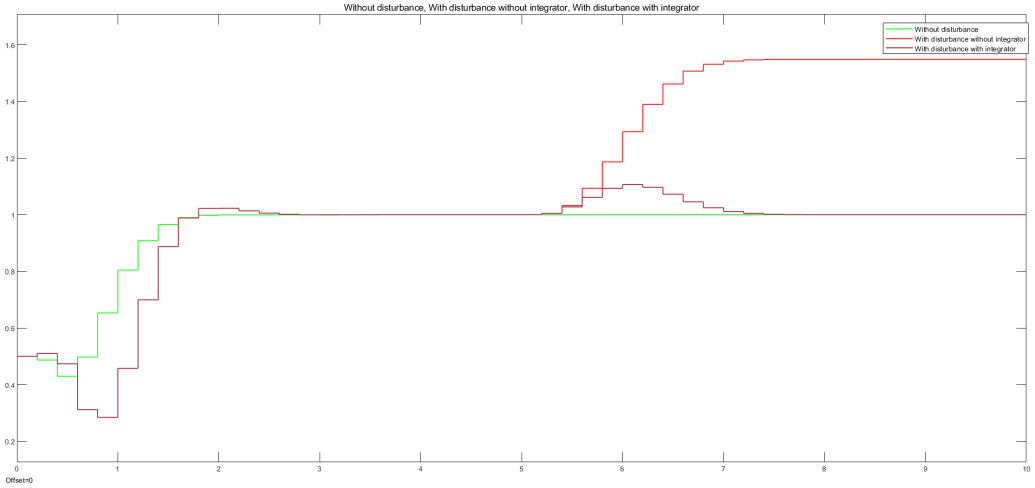

Figure 17: Performance of disturbance rejection among systems

2.5 Question 7: LQ Controller

LQ control, standing for the linear quadratic control is an important control strategy that integrates control engineering and numerical optimization. The block diagram of the LQ-controlled system is the same as figure 16 illustrated. The difference between the pole placement and the LQR is in the way to obtain the feedback gain K.

To acquire gain K for the LQR controller, two weight matrices Q and R are defined to minimize the cost function

$$J = \sum_{k=1}^{\infty} (x_k^T Q x_k + u_k^T R u_k) \tag{27}$$

follows by obtaining a buffer variable P by solving the discrete Riccati equation

$$A^T P + PA - (PB + N)R^{-1}(B^T P + N^T) + Q = 0 \tag{28}$$

finally, the feedback gain K is obtained by

$$K = R^{-1}(BP + N^T) \tag{29}$$

From the definition of the cost function 27, it can be concluded that Q and R are corresponding weight matrices to states x and input u, and the dimension of both square matrices should be the same as the dimension of X and u. Entry q_{ij} denotes the influence of the interaction between x_i and x_j. For this assignment, matrix Q is set to a diagonal matrix with the form of

$$Q = \begin{bmatrix} q_{11} & 0 & 0 \\ 0 & q_{22} & 0 \\ 0 & 0 & q_{33} \end{bmatrix} \tag{30}$$

The gains are obtained by using the *dlqr* function in Matlab. The i^{th} element on the diagonal represents the weight to penalize state x_i, whose value has a positive relationship with the extent of penalty exerted on state x_i. The larger the entry, the more state x_i is penalized, which eventually results in a smaller value of x_i. The same analogy can be posed on the relationship between weight matrix R and input u.

To see the relation between the choice of Q and R to the final reference tracking result, six different combinations of weight matrices are selected as table 2 listed as well as its corresponding discrete closed-loop pole positions, and feedback gain K.

Name	R	Q	K	Closed-loop pole
Gain1	1	diag(1 1 1)	[0.0166 -0.0211 0.0091]	0.0002, 0.9827±0.0098i
Gain2	1	diag(1 1 1000)	[0.0836 0.010 0.4915]	0.0002, 0.9199±0.073i
Gain3	1	diag(0.01 0.01 1000)	[0.3538 0.0121 4.0752]	0.0151, 0.7533±0.195i
Gain4	1	diag(0.001 0.001 1000)	[0.5814 0.0131 9.4604]	0.1162, 0.5835±0.287i
Gain5	0.1	diag(0.001 0.001 1000)	[0.6377 0.0143 10.6427]	0.015, 0.5783±0.2836i
Gain6	10	diag(0.001 0.001 1000)	[0.4000 0.0094 5.8100]	0.3849, 0.6278±0.2954i

Table 2: Different combinations of weight matrices and its corresponding gain K and closed-loop poles position

The step responses of systems with different selection of Q and R are illustrated in figure 18

Recall the physical meaning of states, from the above demonstrations, several conclusions can be drawn based on the change of patterns:

- Observed from gain 1 to gain 4: When R holds the same, by penalizing the x_3 (the heading of the aircraft) more, the step response of the system becomes faster. This can also be noticed by the positions of the closed-loop poles becoming closer to the origin as q_{33} increases.
- Observed from gain 4 to gain 6: When Q holds the same, decrease R accelerate the system's response. An explanation for this phenomenon is that the magnitude of control input u is in reverse relationship with the magnitude of R. As a result, when R is kept very large, the amount of control exerted on the system is small, resulting in a slow response. This can also be noticed by the position of the closed-loop poles.
- The most ideal combination of Q and R will be:
  - Q with a large q_{33}, and small q_{11} and q_{22}
  - R with a very small value

  However, everything comes with a price. The perfect combination leads to a super large gain of K. Thus, a trade-off is indispensable to be found between the control effect and the feasibility.

Lastly, to validate the assumption that the magnitudes of variables are in reverse relationship with corresponding the magnitudes of the penalty terms, x_1, x_2, and x_3 are plotted with different gains in figure 19, from which we observed the expected pattern.

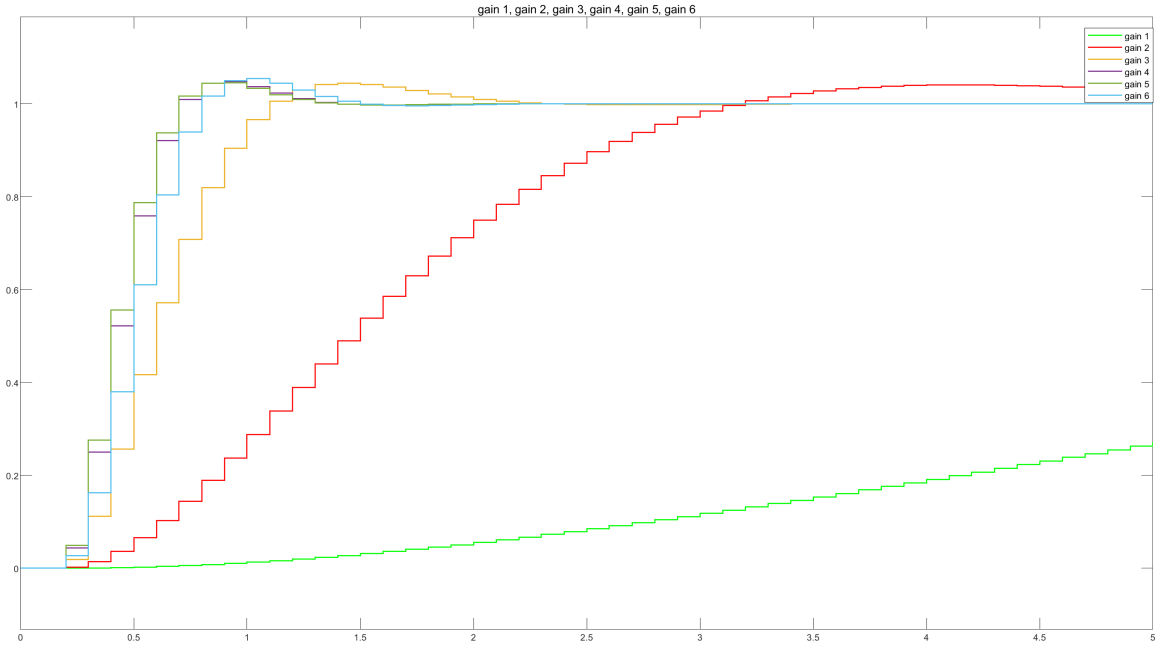

Figure 18: Step response of systems controlled by different LQR gain K

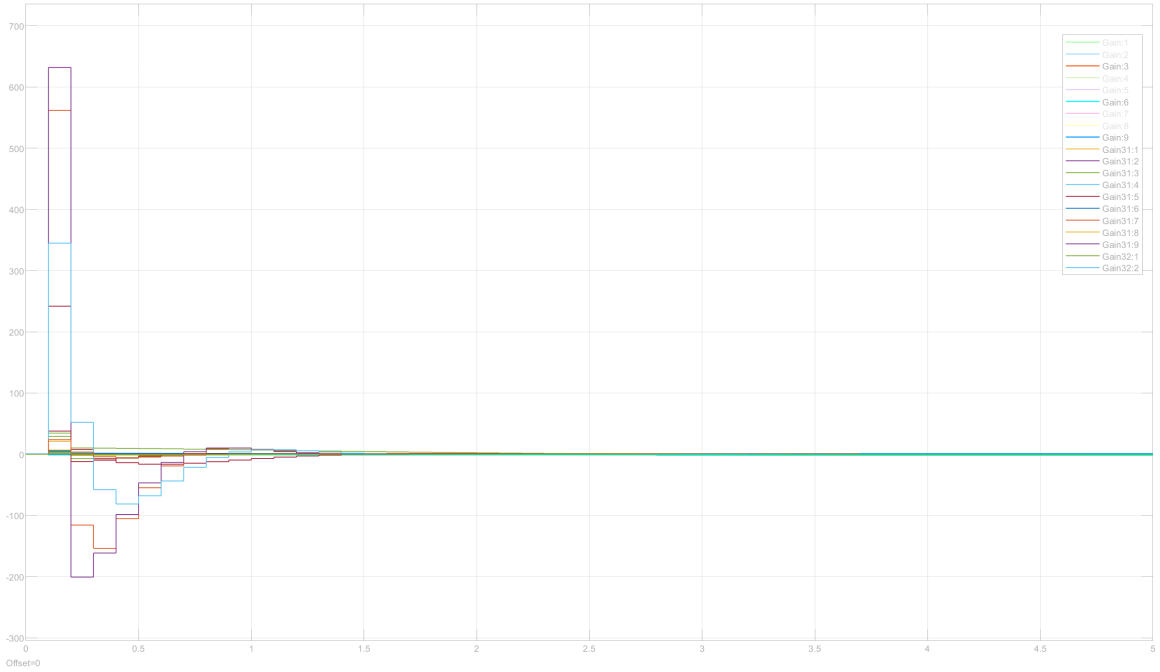

Figure 19: Magnitude of different states when applying different magnitude of feedback gain K

Finally, the selected combination of R and Q is **Gain5**:

$$R = 0.1$$

$$Q = \begin{bmatrix} 10^{-3} & 0 & 0 \\ 0 & 10^{-3} & 0 \\ 0 & 0 & 10^{3} \end{bmatrix}$$

3 Control Design with Limitations

In section 1 and section 2, no limitations are added to either control input u or state x. However, in the real engineering scenario, it is certainly not the case. Thus, this chapter serves to mimic those situations by investigating the effects of limiting the magnitude of the control signal on the performance of the control loop.

3.1 Question 8: Compute Controllers Input

In this chapter, the input to the system u is calculated and visualized. Moreover, it is expected that the magnitude of inputs should exceed ± 1 for both reference tracking and disturbance rejection while satisfying the requirements.

3.1.1 Discrete PID Controller

In this chapter, the system inputs for discrete PID controllers are computed and visualized. To compute u, the transfer functions for reference tracking and disturbance rejection are utilized, resulting in the z transformation of u be defined as

$$U(z) = \frac{C(z)}{1 + C(z)G(z)}Y(z) \tag{31}$$

for reference tracking, and

$$U(z) = \frac{1}{1 + C(z)G(z)}Y(z) \tag{32}$$

for disturbance rejection.

The computed input is visualized in figure 20.

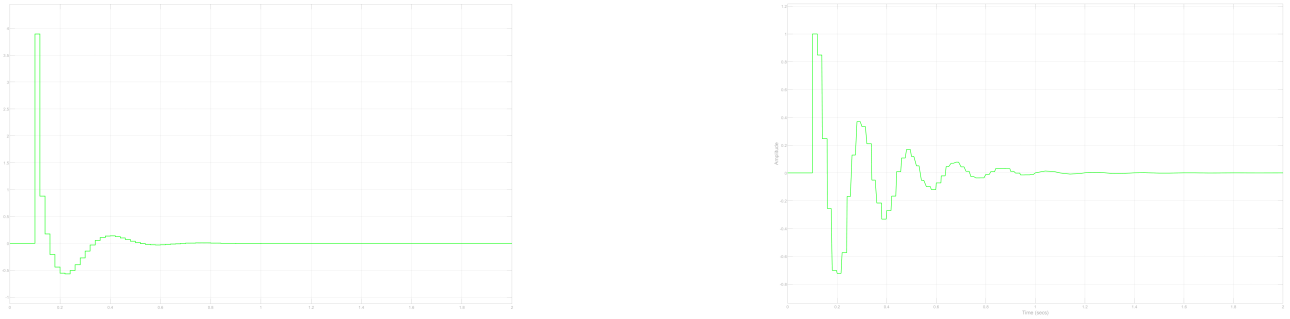

(a) Reference Tracking

(b) Disturbance Rejection

Figure 20: System input of discrete PID

3.1.2 Servo Pole-placement Controller

When constructing the servo controller using pole placement, the control input u is defined as equation 24. Thus, the control input can be computed given state x and reference r. The system input is visualized below in figure 21.

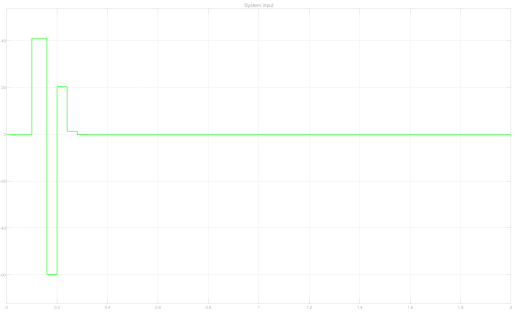

Figure 21: System input of the pole placement controller

3.1.3 Observer-integrated Controller

When an observer is integrated into the system, the corresponding system input u becomes not determined by x and r as in equation 24 but $\hat{x}$ and u. As a result, the u for the system becomes

$$u(k) = -K\hat{x}(k) + K_r r(k) \tag{33}$$

for reference tracking, and

$$u(k) = -K\hat{x}(k) + \hat{\omega}(k) + K_r r(k) \tag{34}$$

for augmented disturbance rejection.

The control inputs for both situations are visualized below in figure 22

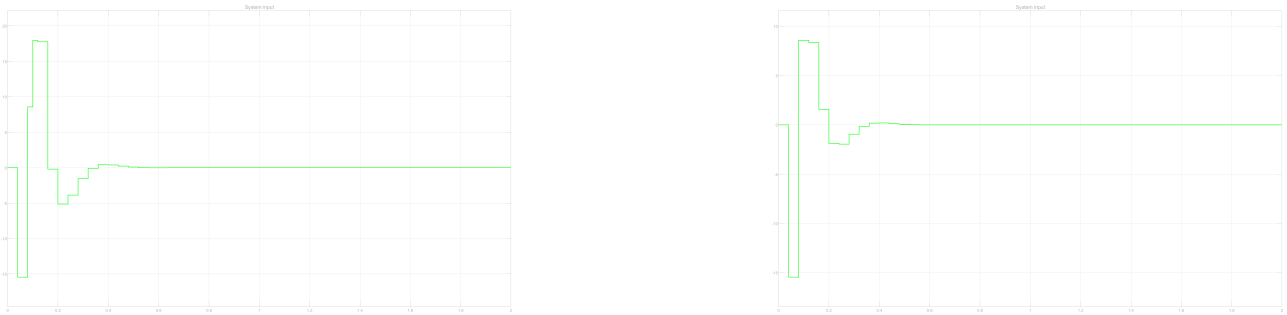

(a) Reference Tracking

(b) Disturbance Rejection

Figure 22: System input of integrated-observer system

3.1.4 LQ Controller

Finally, the computation of system input u for the LQR system is the same as equation 24 with K representing the feedback gain acquired from solving equation 28 instead of pole placement.

The system input of the LQR-controlled system is visualized below in figure 23.

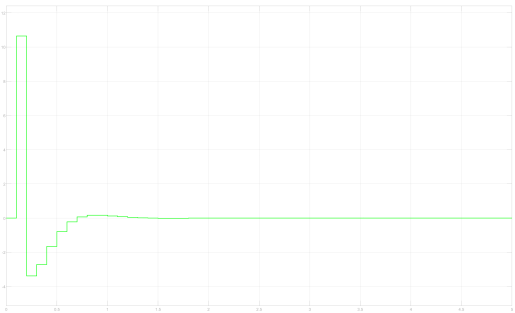

Figure 23: System input of the LQR controller

3.2 Question 9: Redesign the PID Controller

In this chapter, the discrete controller for reference tracking and disturbance rejection is redesigned to meet the limitation for the magnitude of input u. Note that in order to simulate the real engineering scenario, changes for the controllers are kept as small as possible for cost-saving purposes.

3.2.1 Reference Tracking

A PD controller was originally designed to achieve reference tracking. From the relation of control output u and k_p and k_d represented at equation 7, the magnitude of u is in a linear positive relation with the magnitude of k_p and k_d. Hence, according to the maximum value of u, a first attempt is made to linearly scale down

the magnitude of both k_p and k_d by $\frac{max(u_o)}{1}$, resulting in $k_p = 0.12$, $k_d = 0.02$, while T_f is kept the same as 0.01.

By doing so, the magnitude limitation is fulfilled for system input u. Subsequently, some minor fine-tunings are performed to improve the step response of the system. It has been proven in chapter 1 that increasing k_p accelerates the system's response while increasing k_d will eliminate oscillations and overshoot. Thus, k_p and k_d are all slightly increased to accelerate the response speed as well as to eliminate oscillations and overshoot. The changing value of controllers and corresponding step response metrics are shown in the table 3.

	Controller Parameters	Closed-loop poles	Overshoot	T_r(s)
Original	$k_p = 0.49, k_d = 0.08$	0.1248,0.9102,0.7625±0.2691i	1.368%	0.1099
Redesigned	$k_p = 0.14, k_d = 0.015$	0.1331,0.9387,0.7699±0.039i	0%	0.6806

Table 3: Comparison of original and redesigned PD controller

The step response and magnitude of u are shown in figure 24. Note that a broken line is also plotted in the figure for reference 1.

(a) Reference Tracking effect

(b) Magnitude of u

Figure 24: Reference tracking effect and magnitude of u of original controller and redesigned controller

Moreover, the visualization of the new closed-loop system is presented in

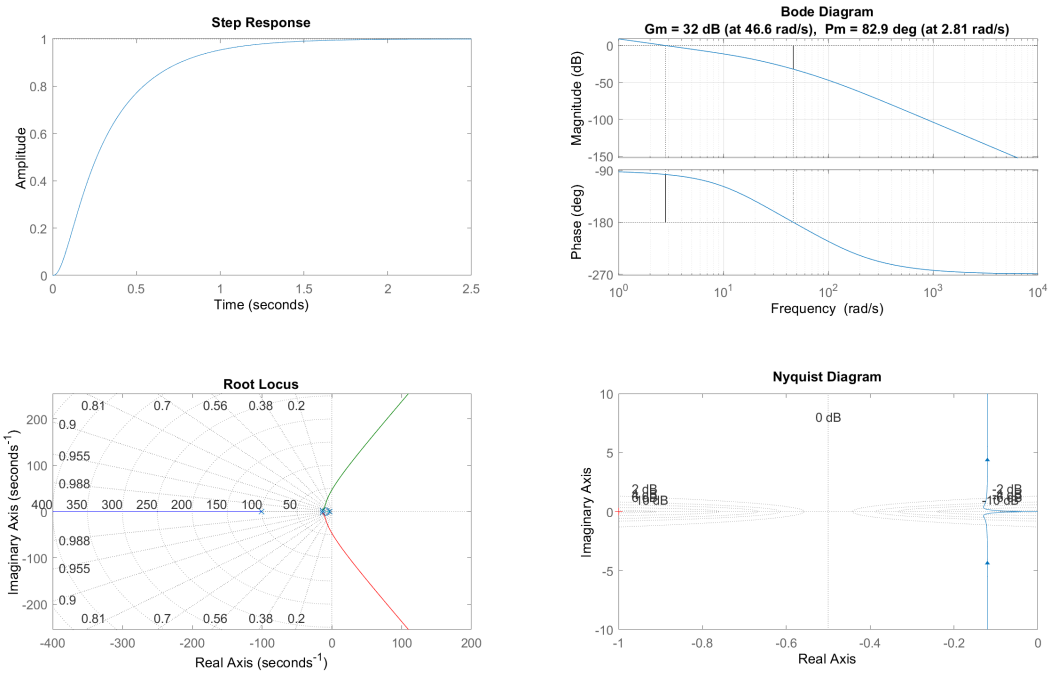

Figure 25: Step response, Bode diagram, Root Locus, and Nyquist Diagram for the newly redesigned system

First, from figure 24, the newly adjusted PD controller fulfills the requirement for its output u under the price of a slower step response. Compared to the original closed-loop system visualized in figure 4, this can be explained by the smaller gain margin and phase margin, as well as the more right position of the closed-loop poles. In the discrete-time domain, this is further proved by the fact that the poles are further to the origin.

3.2.2 Disturbance Rejection

According to figure 20, the u of the PID controller designed for disturbance rejection already fulfills the requirement. Hence, there is no need to redesign the controller.

3.3 Question 10: Redesign the Pole Placement Controller

In the original design, the poles of the system are put radically near the origin in the unit circle since there is not any limitation. This choice of pole positions results in a very large value of gain k, which leads to a large value of system input u. Thus, the effort is mainly focused on making the poles less radical for a small gain k.

When placing the poles, the three poles of the system are divided into a real pole and a pair of conjugated pairs. When placing the new poles, I adopted the same logic. The real pole of 0.01 is kept the same to guarantee the fast system's response, while the conjugated poles are redesigned by moving them farther from the origin. For tuning, the real part of the conjugated pole is first increased while the imaginary part is held as constant. This reaction results in a decreasing system input value u. However, increasing the real part while holding the imaginary part of the pole increases the damping ratio ζ, resulting in the overdamped system response. Thus, the imaginary part is decreased accordingly to achieve a better transient response by approaching to critically damped situation.

After a few attempts, the final pair of poles are selected. Compared to the original poles, the changing of the discrete poles, and their corresponding continuous poles, gain K, overshoot, and rise time T_r is shown in table 4.

	Discrete Pole	Continuous Pole	K	Overshoot	T_r(s)
Original	0.01,0.01±0.1i	-230.26,-114.88±73.56i	[1.5574,0.021,41.0051]	0%	0.0221
Redesigned	0.01,0.9±0.085i	-230.26,-5.05±4.71i	[0.1151,0.0101,0.7134]	0.5122%	0.3226

Table 4: Comparison of original and redesigned Pole Placement controller

The step response and magnitude of u are shown in figure 26. Note that a broken line is also plotted in the figure for reference 1.

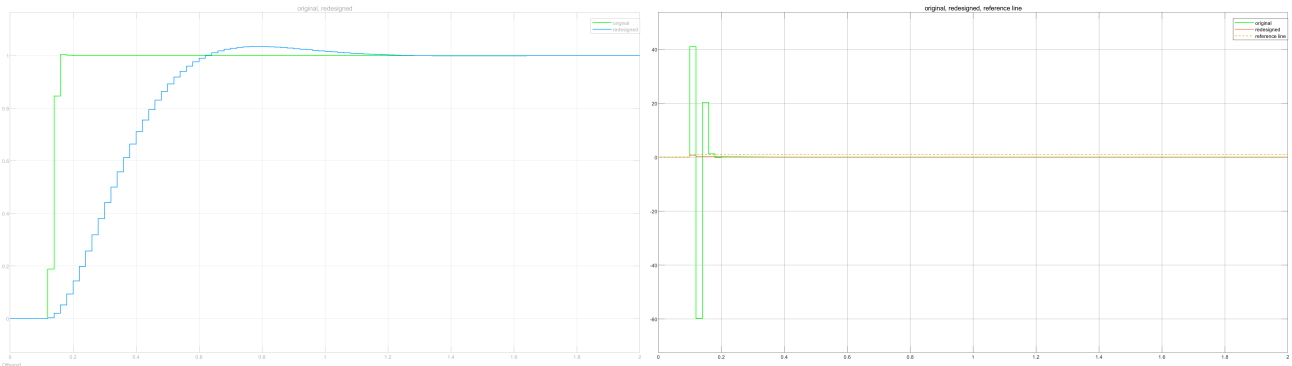

(a) Reference Tracking effect

(b) Magnitude of u

Figure 26: Reference tracking effect and magnitude of u of original controller and redesigned controller

In the context of the redesigned system illustrated in Figure 26, it becomes evident that the magnitude of the control signal, denoted as u, is now constrained to values smaller than 1. This adjustment comes as part of a deliberate trade-off, resulting in a slower step response accompanied by a controlled overshoot. The rationale behind this observation lies in the strategic relocation of the system's poles to positions farther from the original configuration, coupled with a reduction in the damping ratio ζ.

3.4 Question 11: Redesign the LQR Controller

Lastly, the LQR controller is redesigned. Based on the analysis done in chapter 2, the magnitude of u has a reverse relationship with the magnitude of the weight matrix R. Hence, attempts are made to tune the system by increasing the value of R while slightly increasing some entries in Q to eliminate overshoot.

Following several iterations, a discernible pattern emerges. Elevating the value of R induces a reduction in the gain k, leading to a diminished control signal, u. However, this adjustment comes at a cost—introducing an overshoot to the system and consequently slowing down the step response. Conversely, augmenting the matrix Q, with a particular emphasis on enhancing entry q_{33} associated with the aircraft's heading weight, facilitates an increase in the gain k. This, in turn, yields a more rapid system response.

Compared to the original poles, the changing of the discrete poles, their corresponding continuous poles, and gain K are shown in table 4.

	R	Q	K	Discrete Poles
Original	0.1	diag([10^{-3},10^{-3},10^{3}])	[0.6377,0.0143,10.6427]	0.015,0.5783±0.2836j
Redesigned	750	diag([10^{-3},10^{-3},10^{3}])	[0.1056,0.003,1.0149]	0.6328,0.802±0.1639j

Table 5: Comparison of original and redesigned LQR controller

The step response and magnitude of u are shown in figure 27. Note that a broken line is also plotted in the figure for reference 1.

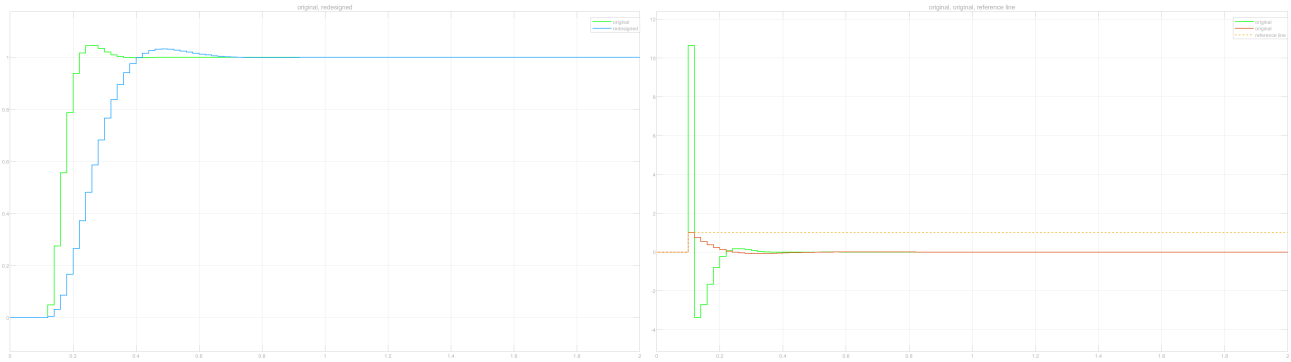

(a) Reference Tracking effect

(b) Magnitude of u

Figure 27: Reference tracking effect and magnitude of u of original controller and redesigned controller

In Figure 27, it is evident that the redesigned controller successfully meets the criterion of restricting the system input, denoted as u, to values not exceeding 1. However, achieving this comes with certain trade-offs. Upon examining the step response, it becomes apparent that the system under the influence of the redesigned LQR controller exhibits a slower reaction. This deceleration can be attributed to the reduced gain applied to the system and the positioning of the poles farther from the origin. Despite this, it's noteworthy that the redesigned system's poles maintain a damping ratio of approximately $\zeta = 0.9797$, a notable improvement from the original system's $\zeta = 0.8978$. This heightened damping effect effectively mitigates any overshooting tendencies within the system.

Indeed, while it holds true that additional fine-tuning could potentially yield enhanced performances from the controllers, it's imperative to revisit the initial premise outlined at the onset of this chapter. The redesign of the controller was undertaken in a manner mirroring real-world engineering scenarios, where adjustments are deliberately kept as minimal as possible. This approach aligns with the practical consideration of cost-saving measures, emphasizing a pragmatic balance between optimization and economic efficiency.

4 Steady-State Error Elimination (Question 12)

In this chapter, I introduce a step disturbance applied to the input, distinct from the step reference. This additional factor has the potential to result in a non-zero steady-state error. Consequently, I present various approaches, either newly proposed or summarized if already available, for discrete Proportional-Integral-Derivative (PID), state feedback, and Linear Quadratic Regulator (LQR) control.

4.1 Theoretical Analysis

Based on the findings from preceding chapters, it is evident that all the controllers exhibit no issues with non-zero steady-state error in terms of reference tracking. However, it is crucial to note that this conclusion does not extend seamlessly to disturbance rejection, necessitating the reconsideration and redesign of specific controllers. The theoretical analysis supporting these adjustments is presented below. Note that the analysis is done in the continuous time domain for demonstration. A block diagram with both reference and disturbance is shown in figure 28 Based on the above figure, define the loop transfer function as $L(s) = C(s) \times P(s)$, then the output

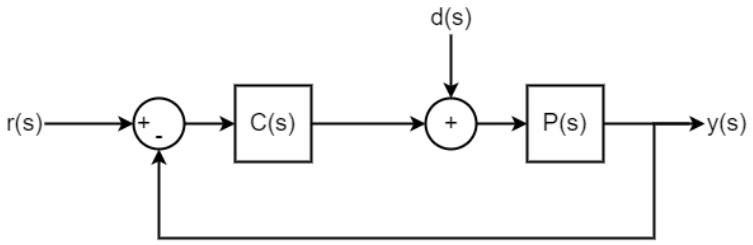

Figure 28: The block diagram of a closed-loop control system with reference $r(s)$ and input disturbance $d(s)$

of the system can be represented as

$$y(s) = \frac{L(s)}{1 + L(s)} r(s) + \frac{P(s)}{1 + L(s)} d(s) \tag{35}$$

By replacing s in equation 35 with $i\omega$, the input-output relationship is acquired in the frequency domain. In order for the system output y equals r under the influence of d, the loop transfer function $L(i\omega)$ should be as large as possible, ideally infinity, so that term $\frac{L}{1+L}$ equals 1 while term $\frac{P}{1+L}$ equals 0, resulting in reject the disturbance $d(s)$. Thus, a high loop gain is the goal of all the designs of our controllers. Furthermore, according to the final value theorem, it is imperative to introduce at least one integrator in the loop transfer function, denoted as $L(s)$. This necessity underscores the augmentation of the system with an additional state, particularly for systems employing state feedback or output feedback control strategies. Lastly, in the realm of controller design, a trade-off must be carefully considered between reference tracking and disturbance rejection. This is because the former generally demands substantial margins, whereas the latter calls for more conservative, smaller margins.

To summarize, the three requirements for designing the system would be:

1. Possibly a large gain to the system
2. At least one integrator in $L(s)$
3. big margins for reference tracking, and small margins for disturbance rejection

4.2 Discrete PID

The PD controller developed in Chapter 2 effectively tracks the reference step signal in the absence of an input disturbance. However, upon introducing a step disturbance into the block diagram, as illustrated in Figure 28, the system exhibits a steady-state error. This occurrence can be attributed to the absence of an integrator in the system, leading to a significant impact of the disturbance on the closed-loop system. Consequently, the PD controller undergoes an upgrade to a PID controller. Adhering to the principle of minimal changes, alterations in this chapter are kept to a minimum. Building upon the PD controller, an integral (I) term is incorporated, and the impact on reference tracking in the presence of disturbance $d(z)$ is depicted in Figure 29.

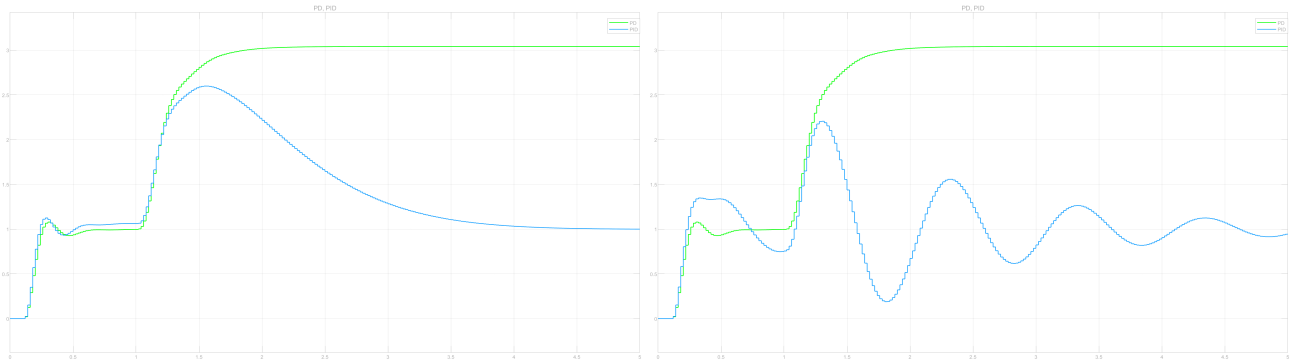

(a) PID with a small k_i (b) PID with a large k_i

Figure 29: Reference tracking of the system controlled by the PID controller with a large and small k_i

In figure 29, the green line stands for the system controlled by the PD controller while the blue line represents the system controlled by the PID controller. One can observe that adding an I term does solve the problem. Moreover, the choosing of k_i is important, since a small k_i makes the system super slow for response, while a large k_i introduces oscillations to the system that could eventually break the stability. The final value for the controller is

	k_p	k_i	k_d
Original	0.49	0	0.08
Redesign	0.5	0.8	0.1

Table 6: Parameters for the PD and PID controller

with the PID defined as

$$PID = K_P + K_I T_s \frac{1}{z-1} + K_D \frac{N}{1 + NT_s \frac{1}{z-1}} \tag{36}$$

The final control effect is shown in figure 30 with $T_s = 0.02s$.

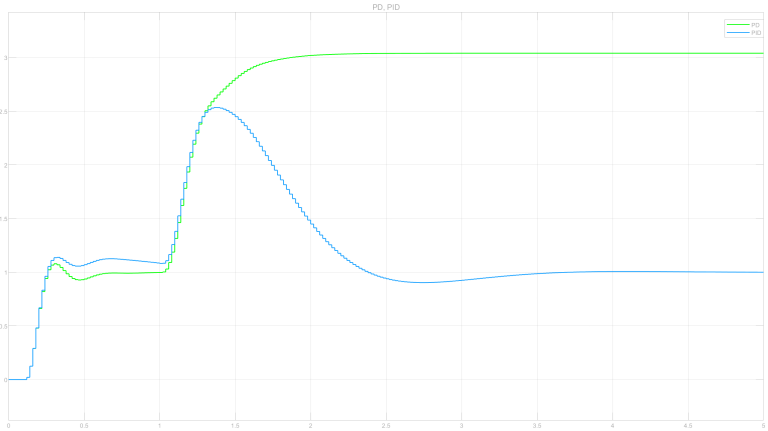

Figure 30: Final control effect of the redesigned PID controller with an input disturbance

4.3 State Feedback

This part has been already answered in chapter 2. To sum up:

- Reference tracking without disturbance: This can be accomplished by strategically placing the poles of the closed-loop system in specific positions. For the discrete system, these poles should be situated within the unit circle, while for the continuous system, they should be on the left-hand side of the plant.
- Reference tracking with disturbance: This can be accomplished by augmenting the system with an extra term since the input to the system becomes $u^{'}(k) = u(k) + d(k)$

The state space representation of the augmented system can be represented as

$$\begin{bmatrix} x(k+1) \\ d(k+1) \end{bmatrix} = \begin{bmatrix} \Phi & \Gamma \\ 0 & 1 \end{bmatrix} \begin{bmatrix} x(k) \\ d(k) \end{bmatrix} + \begin{bmatrix} \Gamma \\ 0 \end{bmatrix} u(k)$$

$$y(k) = \begin{bmatrix} C & 0 \end{bmatrix} \begin{bmatrix} x(k) \\ d(k) \end{bmatrix}$$

$$u(k) = \begin{bmatrix} -k & -k_\omega \end{bmatrix} \begin{bmatrix} x(k) \\ d(k) \end{bmatrix} + K_r r(k)$$

Since not all states are observable, an observer is added in chapter 2 to estimate state x and new state d, the corresponding closed-loop with an observer can be represented as

$$\begin{bmatrix} x(k+1) \\ d(k+1) \\ \hat{x}(k+1) \\ \hat{d}(k+1) \end{bmatrix} = \begin{bmatrix} \Phi & \Gamma & 0 & 0 \\ 0 & 1 & 0 & 0 \\ LC & 0 & \Phi - LC & \Gamma \\ L_d C & 0 & -L_d C & 1 \end{bmatrix} \begin{bmatrix} x(k) \\ d(k) \\ \hat{x}(k) \\ \hat{d}(k) \end{bmatrix} + \begin{bmatrix} \Gamma \\ 0 \\ \Gamma \\ 0 \end{bmatrix} u(k)$$

$$y(k) = \begin{bmatrix} C & 0 & 0 & 0 \end{bmatrix} \begin{bmatrix} x(k) \\ d(k) \\ \hat{x}(k) \\ \hat{d}(k) \end{bmatrix}$$

$$u(k) = \begin{bmatrix} -k & -k_d \end{bmatrix} \begin{bmatrix} \hat{x}(k) \\ \hat{d}(k) \end{bmatrix} + K_r r(k)$$

The control effect is visualized in figure 17.

4.4 Linear Quadratic Regulator

The LQR-controlled system is quite similar to the state feedback one since LQR is just another way of obtaining feedback gain K. Hence, the design can also be split into two minor tasks

- Reference tracking without disturbance: This can be accomplished by choosing a nice Q and R so that state x and input u are penalized accordingly, resulting in placing the closed-loop poles in the proper position (within the unit circle for the discrete system).
- Reference tracking with disturbance: An augmented state should be added to the system. This can be done as the previous sub-chapter shows, by augmenting the system based on the input change or adding an integrator to the system.

I tried to augment the system using an integrator for LQR instead of copying the work from the state feedback. Subsequently, the state space representation for the augmented system becomes

$$\begin{bmatrix} x(k+1) \\ x_{aug}(k+1) \end{bmatrix} = \begin{bmatrix} \Phi & 0 \\ -C & 1 \end{bmatrix} \begin{bmatrix} x(k) \\ x_{aug}(k) \end{bmatrix} + \begin{bmatrix} \Gamma \\ 0 \end{bmatrix} u(k)$$

$$y(k) = \begin{bmatrix} C & 0 \end{bmatrix} \begin{bmatrix} x(k) \\ x_{aug}(k) \end{bmatrix}$$

$$u(k) = \begin{bmatrix} -k & -k_{x_{aug}} \end{bmatrix} \begin{bmatrix} x(k) \\ x_{aug}(k) \end{bmatrix} + K_r r(k)$$

One can notice the definition of augmented system matrix A_{aug} changes dramatically compared to the augmentation method I adopted at the state feedback. This is mainly because the augmented state, the integrator, is decoupled from input $u(k)$ with only a relationship established with state $x(k)$. Instead, the augmented state represents the error $q = r - y = r - Cx$. Moreover, it is noteworthy to mention that, for designing the LQR, I assumed that all the states of the system are observable so there is no need to design an observer.

Since it is the LQR controller, the feedback gain K should be acquired by tuning the Q and R matrices. However, tuning these matrices can be very indirect. So the poles are placed directly. To guarantee the fast response of the system, the poles are chosen. The final chosen poles and the corresponding gain are shown in table 7.

Poles	Gain K
[0.5783±0.2836i,0.2,0.1]	[1.1905,0.0183,35.6029,-7.7788]

Table 7: Final choice for pole and the corresponding feedback gain

The corresponding final result for control is illustrated in figure 31. In the simulation, a zero reference r is given to the system while an input disturbance d with the magnitude of 5 is exerted on the system at the very start. Consequently, the anticipated behavior entails the system sustaining a zero output, even in the presence of d.

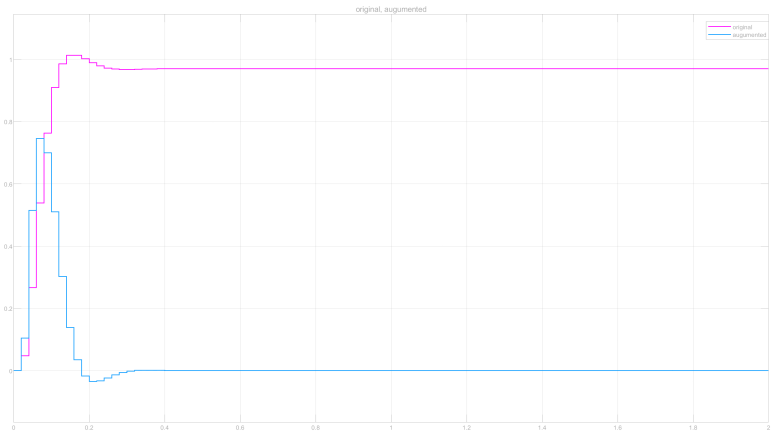

Figure 31: The control effect of the LQR system and the augmented LQR system

Observing Figure 31, it becomes evident that the augmented LQR consistently maintains an output value of 0, fulfilling the expected behavior. In contrast, the original system falls short of meeting these expectations. Consequently, it can be reasonably concluded that the system effectively rejects the disturbance, achieving zero steady-state error.

To summarize

Control Method	Task	Steady-State Error Elimination Method
Closed-loop feedback (PID)	Reference Tracking	1 integrator in the system
	Disturbance Rejection	1 integrator in the system
State Feedback	Reference Tracking	Place poles in proper positions
	Disturbance Rejection	1 integrator argument to the system

Table 8: Summary of methods to achieve zero steady-state error

5 Control Design with Delays

In many scenarios, the assumption is often made that the system operates without any delay. However, when dealing with real-world plants, such as a car, delays become prevalent due to multiple generating sources. It becomes crucial to meticulously consider these delays, as they can induce substantial alterations to the system's dynamics. This chapter is dedicated to replicating such real-world scenarios. Subsequently, a delay is introduced to the system. Furthermore, the initial controllers are evaluated based on their performance and adjusted as needed.

5.1 PID Controller

In the discrete-time domain, adding a time delay to the system indicates a change to its transfer function. To be more specific, the transfer function of the plant becomes

$$G_{new}(z) = \frac{G(z)}{z} \tag{37}$$

which leads to the corresponding change in the closed-loop transfer function of the system. The theoretical knowledge of control tells that the addition of time delay, which has the same effect as adding an integrator to the system, could lead to more overshoot and oscillations to the original response. Consequently, it is anticipated that re-calibration of controller parameters becomes imperative for effective reference tracking and disturbance rejection. Lastly, since all the control designs are done in Simulink, it is worth mentioning that the block diagram changes accordingly as figure 32 shows.

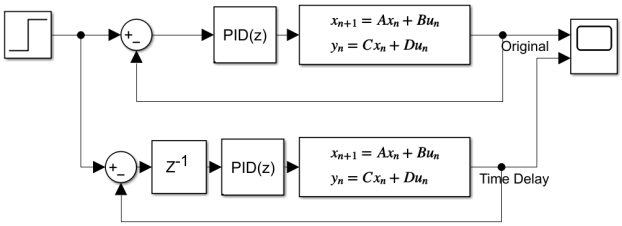

Figure 32: Bloack diagram of PID controlled system with and without time delay

5.1.1 Reference Tracking

The step response of system with and without time delay z^{-1} is visualized in figure below From the visual-

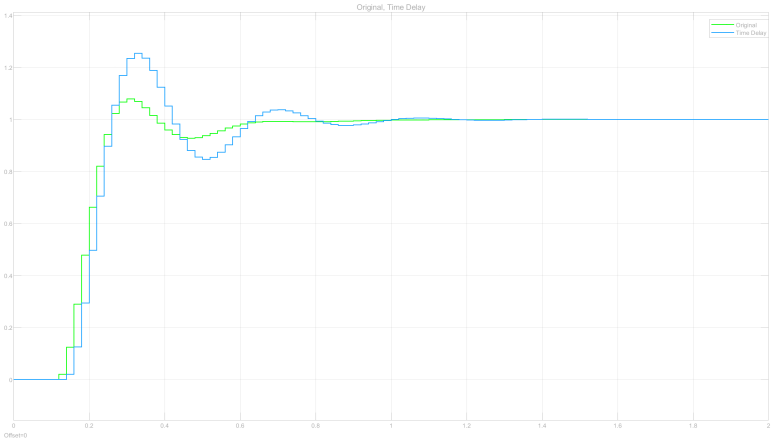

Figure 33: Step response of the system with and without time delay

ization, it can be seen that the system with a time delay has a larger overshoot and oscillations compared to the system without a time delay. This observation justifies our prediction when analyzing the change in plant transfer function after adding a time delay. Moreover, adding a time delay does not change the stability of the

original system, which only leads to some minor changes to the original PD controller.

To decrease the overshoot and oscillations, k_p is decreased as well as the k_d. Hence, the redesigned controller parameters become

	k_p	k_i	k_d	Overshoot	$T_r(s)$
Original	0.49	0	0.08	23.5%	0.22
Redesign	0.4	0	0.05	10%	0.31

Table 9: Original PID and redesigned PID parameters for reference tracking

The step response of the two PID controllers is shown in figure 34

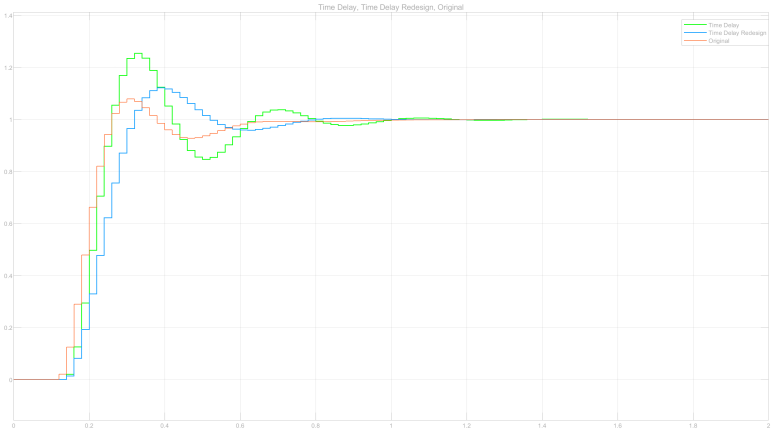

Figure 34: Step response of the original system, time-delay system with original PID, and time-delay system with redesigned PID

It can be observed that the redesigned PID has a better control effect compared to the original PID in the time-delay system, and since k_p and k_d are all decreased, the percentage of overshoot and the extent of oscillations decreased. However, this improvement comes at the expense of a slower response in the system, which can be noticed by the increasing rise time T_r.

5.1.2 Disturbance Rejection

The same delay is added to the PID-controlled system for disturbance rejection, and I got the result of figure 35 shows

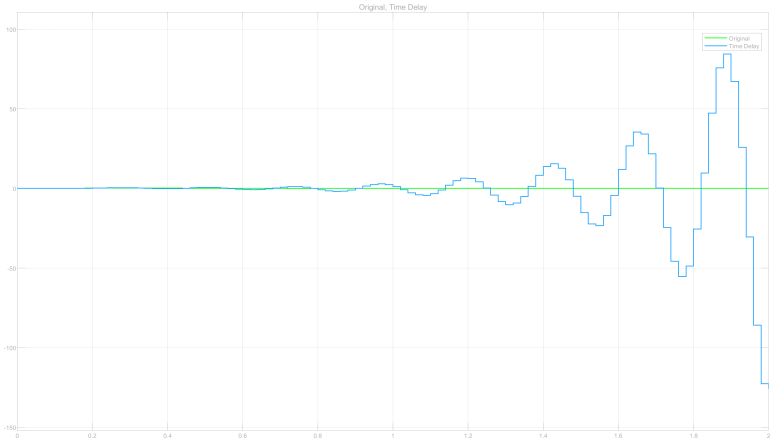

Figure 35: Disturbance rejection result of original PID-controlled system with and without a time delay

It can be seen that the original controller fails to reject the disturbance, and the stability of the system

eventually breaks after 1 second. Hence, a major rework is required to redesign the controller.

To scrutinize the reason behind the performance between, the performance, as well as the bode diagram of the original PID controller in the system with and without time delay is visualized in figure 36

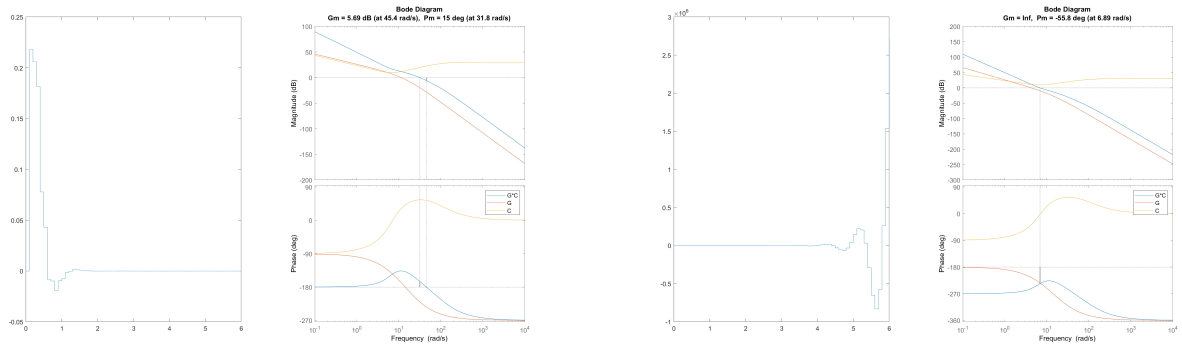

(a) Without time delay

(b) With time delay

Figure 36: The disturbance rejection performance and the bode diagram of PID controlled system with and without time delay

The infinity gain margin and the phase margin of -55.86^o match the observation of instability. From the original starting point of the phase plot and gain plot, the effect of time delay z^{-1} can be seen — By adding a time delay, an integrator is added to the system, so that the phase has a -90^o lag, leading to the instability. Hence, the parameters of the PID are scaled down and adjusted to increase the gain margin and phase margin. Moreover, in order to pursue a good performance for disturbance rejection, the phase margin is kept as small as possible. After a few attempts, the returned PID parameters are shown in the table 10

	k_p	k_i	k_d	T_f
Original	2.9	15	0.3	0.01
Redesign	0.9	0.7	0.3	0.01

Table 10: Original PID and redesigned PID parameters for disturbance rejection

The bode diagram and disturbance rejection effect of the redesigned PID controller are shown in the visualization of figure 37. Note that since the system with a time delay controlled by the original PID controller is unstable, the system without a time delay is used as a comparison.

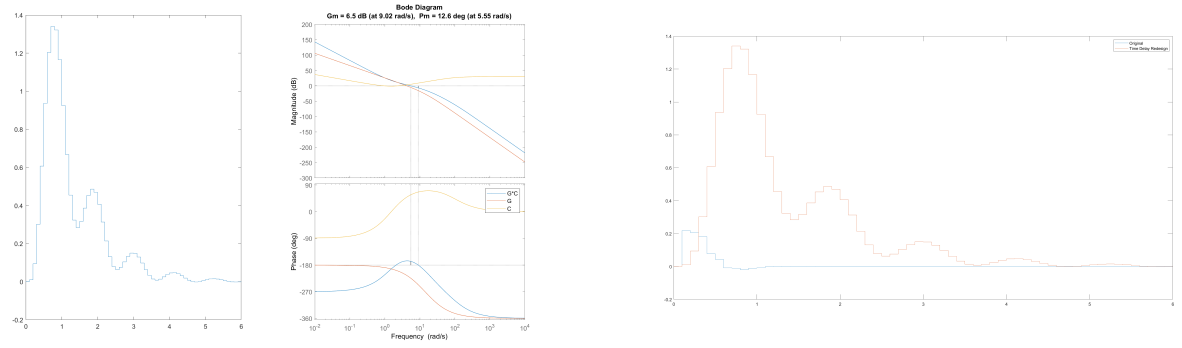

(a) Visualization of redesigned controller

(b) Effect of disturbance rejection

Figure 37: The disturbance rejection performance and the bode diagram of redesigned PID controlled system

In order to achieve a decent disturbance rejection effect, the parameters of the redesigned system are tuned so that the new system has a gain margin and phase margin of $6.5dB$ and 12.6^o, which is close to the value of $5.69dB$ and 15^o of the original system without a time delay. Even with the similar value of phase margin and gain margin, one can still observe that the newly designed system has a large overshoot and oscillation. If

I decrease the k_i and increase the k_d, which are the two most common options to solve this problem, would result in a negative gain margin, leading to instability. This underscores the conclusion that the introduction of a time delay fundamentally alters the inner structure of the system. Lastly, note that the sampling time is kept as $T_s = 0.02s$ for the redesign.

5.2 State Feedback Controller

The focus of the work in Chapter 5.1 primarily revolved around the transfer function representation of the system. However, with the introduction of a time delay, it becomes imperative to reevaluate and redesign the state feedback controllers of the system. Consequently, the efforts in this chapter are primarily directed towards the state space representation of the system.

5.2.1 Reference Tracking

The state space representation of the original system can be found in chapter 2. Note that the definition of u remains the form of equation 24 for the rest of this chapter. When adding a time delay to the system, the state space representation of the system becomes

$$\begin{aligned} x(k+1) &= \Phi x(k) + \Gamma u(k-1) \\ y(k) &= Cx(k) + Du(k-1) \end{aligned}$$

with $D = 0$.

In order to compute and simulate, the system should be written in a form that contains terms $u(k)$ and $u(k-1)$. Hence, similar to the technique adopted in chapter 2, the system should be augmented with an extra term representing the $u(k)$. As a result, the state space representation of a system integrating both the time delay and the state feedback gain can be written as

$$\begin{aligned} \begin{bmatrix} x(k+1) \\ u(k) \end{bmatrix} &= \begin{bmatrix} \Phi & \Gamma \\ 0 & 0 \end{bmatrix} \begin{bmatrix} x(k) \\ u(k-1) \end{bmatrix} + \begin{bmatrix} 0 \\ 1 \end{bmatrix} u(k) \\ y(k) &= \begin{bmatrix} C & 0 \end{bmatrix} \begin{bmatrix} x(k) \\ u(k-1) \end{bmatrix} \\ u(k) &= \begin{bmatrix} -k & -k_u \end{bmatrix} \begin{bmatrix} x(k) \\ u(k-1) \end{bmatrix} + K_r r(k) \end{aligned}$$

Before redesigning the controller, the original state-feedback controller is assessed, when maintaining the first three poles as the non-augmented system and placing the last one arbitrarily, the result of the step response of the system is shown in figure 38.

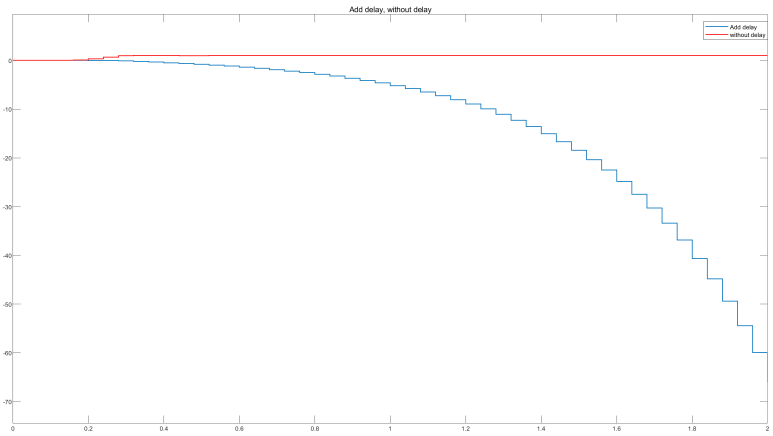

Figure 38: Step response of the state feedback system with and without delay

From figure 38, when adding a time delay, the original system exploded. To solve the problem, and make the performance of the system with time delay resemble the one without time delay, the pairs of poles to be placed are chosen carefully based on the originally placed poles. The very last procedure before placing the pole will be to test the controllability of the augmented system. The controllability matrix is constructed as

$$C_{br} = \begin{bmatrix} B_{aug} & A_{aug}B_{aug} & A_{aug}^2 B_{aug} & A_{aug}^3 B_{aug} \end{bmatrix} \tag{38}$$

The rank of the matrix 38 equals 4, indicating controllability. As a result, 3 sets of poles are chosen. Note that the sampling time is held as $T_s = 0.02s$. The corresponding step response of systems controlled by state

	Discrete Pole	Continuous Poles	Gain K
Original	0.5,0.4±0.5i	-34.66,-22.29±44.80i	[0.6945 0.0114 12.7592]
Pole1	0.5,0.4±0.5i,0.6	-34.66,-22.29±44.80i,-25.54	[0.4735 0.0115 5.1037 0.5891]
Pole2	0.5,0.4±0.5i,0.1	-34.66,-22.29±44.80i,-151.13	[0.8207 0.0172 11.4833 1.0891]
Pole3	0.2,0.2±0.1i,0.1	-80.47,-74.89±23.18i,-151.13	[1.3378 0.0276 19.5780 1.7891]

Table 11: Choice of poles for the redesign RT under the influence of time delay

feedback controllers is shown in figure 39

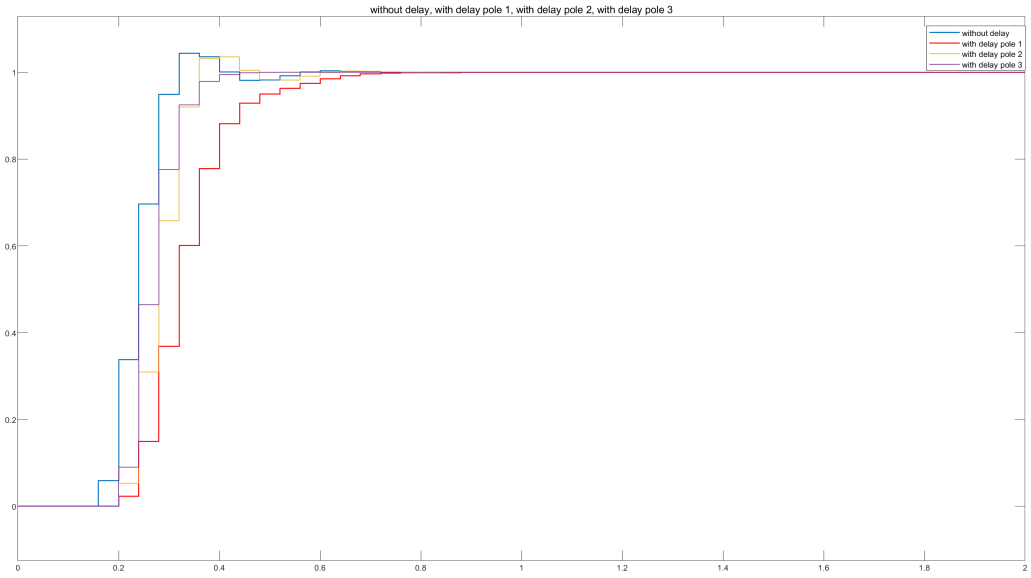

Figure 39: Step response of redesigned PID systems

From figure 39, there are few things can be observed

- When keeping the poles for x the same as the original system. The further the pole for the delay term is placed from the origin, the slower the response of the system.
- When the pole for the delay term is strategically positioned closer to the closed-loop poles, it results in enhanced system performance. This improvement can be attributed to the rapid convergence of the delay unit, effectively minimizing the impact of the delay on the overall system. By facilitating a faster convergence, the delay's influence is mitigated, leading to improved system behavior and performance.
- The closer the poles are to the origin, the faster the system is for the step response. But everything has two coins, the closer the pole to the origin, the larger the gain K becomes. Thus, it is important to find a trade-off between the technical feasibility and the performance of the system.

After considering factors including the behavior of the system and cost to implement, the new controller is designed by placing the pole in the same location as **Pole2**.

5.2.2 Disturbance Rejection

It has been analyzed that an integrator is needed under the existence of an input disturbance d. This is validated by figure 40, which shows the disturbance rejection effect of the system with and without augmentation under the existence of a time delay.

When adding an input disturbance, the original augmented system succeeds in rejecting the disturbance. However, the system with a time delay is greatly influenced and fails to reject. Consequently, the system is augmented in alignment with the time-delay augmentation. Similar to the augmenting techniques adopted in the redesign of the LQR controller to eliminate the steady-state error in chapter 4, an integrator is added to

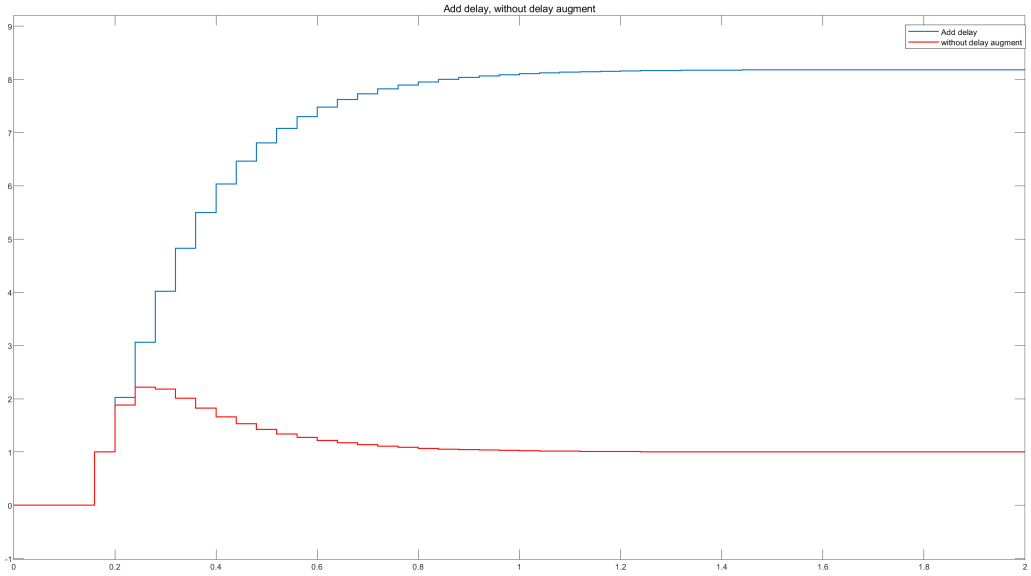

Figure 40: The disturbance rejection effect of the system with and without time delay

the system by augmenting the system with an extra state representing the error of output and the reference. Subsequently, the state space representation of the augmented system becomes

$$\begin{bmatrix} x(k+1) \\ x_{new}(k+1) \\ u(k) \end{bmatrix} = \begin{bmatrix} \Phi & 0 & \Gamma \\ -C & 1 & 0 \\ 0 & 0 & 0 \end{bmatrix} \begin{bmatrix} x(k) \\ x_{new}(k) \\ u(k-1) \end{bmatrix} + \begin{bmatrix} 0 \\ 0 \\ 1 \end{bmatrix} u(k)$$

$$y(k) = \begin{bmatrix} C & 0 & 0 \end{bmatrix} \begin{bmatrix} x(k) \\ x_{new}(k) \\ u(k-1) \end{bmatrix}$$

$$u(k) = \begin{bmatrix} -k_1 & -k_2 & -k_u \end{bmatrix} \begin{bmatrix} x(k) \\ x_{new}(k) \\ u(k-1) \end{bmatrix} + K_r r(k)$$

Prior to the design phase, an evaluation of system observability is conducted to ascertain whether the construction of an observer is required. Accordingly, the observable matrix is formulated as follows.

$$C_{ob} = \begin{bmatrix} C_{aug} \\ C_{aug}A_{aug} \\ C_{aug}A_{aug}^2 \\ C_{aug}A_{aug}^3 \end{bmatrix} \tag{39}$$

The rank of the matrix 39 equals 4, indicating observability. Thus, there is no need to build an observer.

As a result, based on the poles of the original system, 2 sets of poles are placed and assessed for the newly augmented system, with their values in the discrete-time domain, values in the continuous-time domain, and corresponding feedback gain k shown in table 12.

	Discrete Pole	Continuous Poles	Gain K
Original	0.2,0.2±0.1i,0.8	-80.47,-74.89±23.18i,-11.16	[1.2497 0.0188 33.33 -4.3507]
Pole1	0.2,0.2±0.1i,0.8,0.1	-80.47,-74.89±23.18i,-11.16,-115.13	[1.6869 0.0319 34.35 -3.9156 1.9891]
Pole2	0.2,0.2±0.1i,0.12,0.1	-80.47,-74.89±23.18i,-106.01,-115.13	[2.8739 0.0469 84.5775 -17.2287 2.6691]

Table 12: Choice of poles for the redesign DR under the influence of time delay

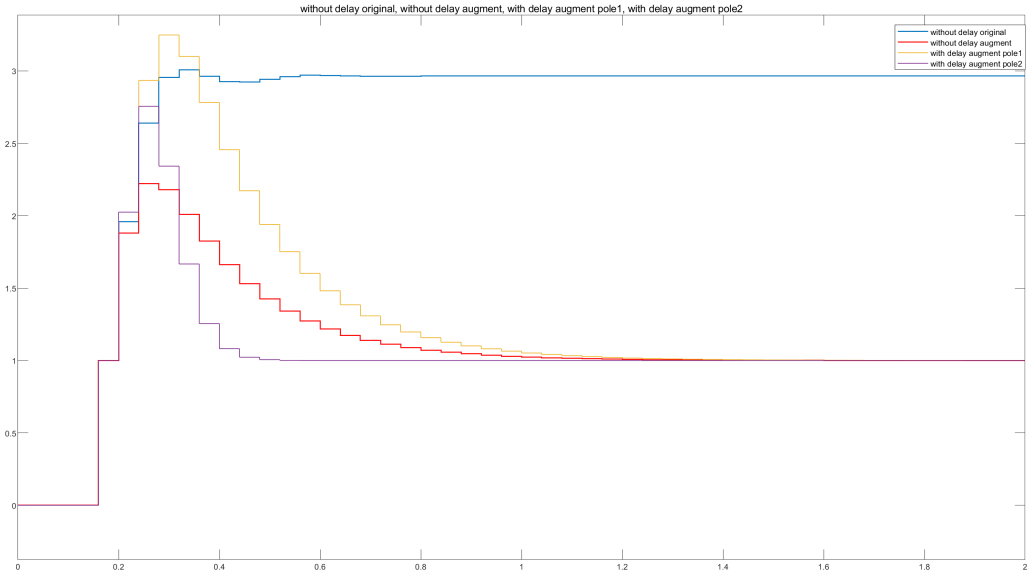

Figure 41: The disturbance rejection effect of the redesigned system with a time delay

Moreover, the disturbance rejection result is shown in figure 41

From figure 41, it can be concluded that the faster the convergence of the time delay term, the better the system is performing disturbance rejection. However, there is the same trade-off to be made between the magnitude of gain k and the system behavior. Eventually, the poles for disturbance rejection are chosen as **Pole2** in table 12.

5.3 LQR Controller

Finally, a time delay is added to the LQR-controlled system. To handle the time delay, an extra state is added to the state space representation of the system. Consequently, the dimension of Q is added from 3 to 4. The reference tracking effect of the system with and without the time delay is shown in figure 42.

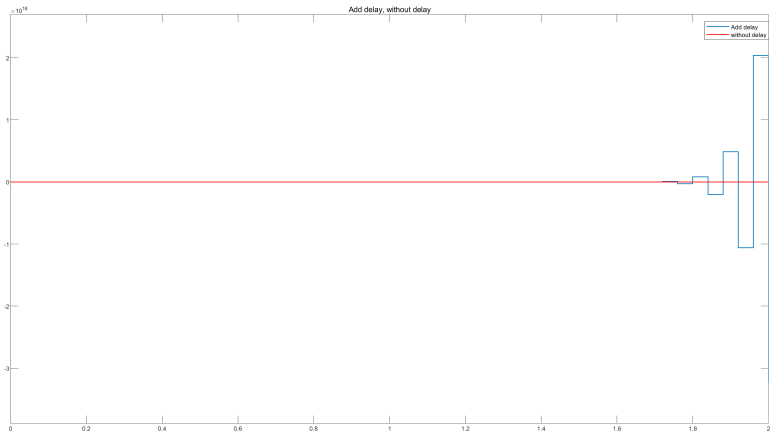

Figure 42: Reference tracking effect of the system with and without the time delay

It can be observed that the system that adopted the original LQR controller exploded within the simulation period, leading to the redesign of the LQR controller.

I have made several multiple attempts to tune the Q and R matrices, yet have encountered challenges without making substantial progress. Consequently, an alternative and indirect methodology has been embraced, in which the desired poles are first placed, and Q and R are approximated based on the selected pole positions. The final positions of poles, and the corresponding weight matrices as well as the gain k are listed in the table below. Additionally, for the sake of comparison, parameters pertaining to the original LQR controller are presented alongside.

	R	Q	Pole positions	Gain K
Original	0.1	diag([10^{-3},10^{-3},10^{3},10^{0}])	[-2.3397±0.6995i,-1.1625,-0.8936]	[2,0.3,199.44,0.92]
Redesigned	10^{5}	diag([10^{-4},10^{-4},10^{-3},10^{-3}])	[-0.5069±0.2i,-04,-0.1]	[5.3405,0.0771,148.8664,4.0029]

Table 13: Parameters of original and redesigned LQR controller

The large overshoot and oscillations in figure 43 can be explained by the large gain k exerted on the system. Hence, fine-tuning can be performed to achieve a better performance. Nevertheless, the redesigned LQR controller succeeds in tracking the given reference under the influence of the time delay.

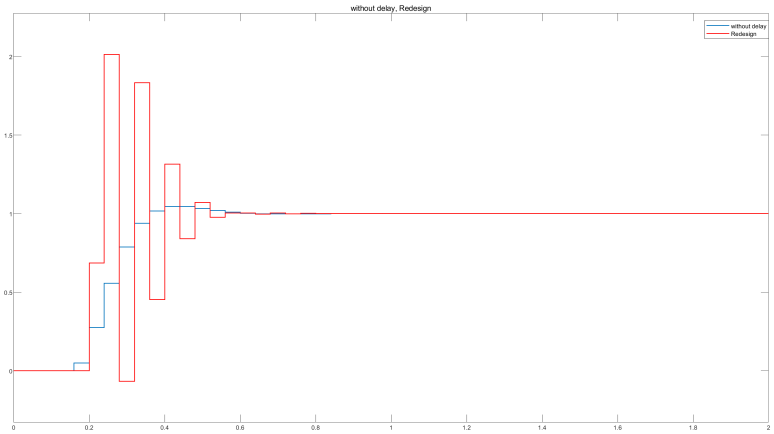

Figure 43: Reference tracking effect of the original and redesigned LQR system with the time delay

6 Conclusion

Through this assignment, the system designated to control the heading of the bi-wing aircraft is designed. The content of the design includes control in both continuous time and discrete time domains in chapter 1 and 2, as well as control using both state feedback and output feedback techniques in those two chapters. All the controllers are examined and adjusted so that no steady-state error is included in chapter 4. In the later part of the report, namely chapter 3 and 5, limitations and time delay are considered. Based on all the theoretical analysis as well as simulation, all the designed controllers meet the performance requirements.

I firmly believe that this assignment serves as an excellent guide, providing individuals with a comprehensive blueprint and overview of control engineering. However, it's crucial to acknowledge that the learning journey in this field is extensive. During my time working part-time as a control and software engineer at Formula Student Team Delft, I gained valuable insights. This experience reinforced the notion that while control is an abstract concept, the design of a control system demands engineers to consider a myriad of practical factors. These include constraints on inputs, speed limitations, latency within embedded systems, and intricate interactions among multiple control loops. Therefore, possessing a commitment to lifelong learning, coupled with a growth mindset, stands as the most crucial arsenal one should wield on this journey.

Concluding this report, there are many trade-offs to be made in terms of design. In this assignment, balances are made in several designs between the performance of the system and the technical feasibility, offering a glimpse into the intricate art of control system design. As a result, it is indispensable to adopt a holistic perspective, steering clear of fixating on individual details, to craft a high-quality, comprehensive system.

References

[1] Karl J. Åström and Björn Wittenmark. *Computer-controlled systems (3rd ed.)* Upper Saddle River, NJ, USA: Prentice-Hall, Inc., Feb. 1997. DOI: 10.5555/248504.

[2] *Control Tutorials for MATLAB and Simulink - Introduction: Frequency Domain Methods for Controller Design*. [Online; accessed 1. Dec. 2023]. Dec. 2023. URL: https://ctms.engin.umich.edu/CTMS/index.php?example=Introduction&section=ControlFrequency#1.

[3] László Keviczky et al. *Control Engineering*. Singapore: Springer Nature, 2019. ISBN: 978-981-10-8297-9. URL: https://link.springer.com/book/10.1007/978-981-10-8297-9.